

**The Fluxgate Electric Field Meter
A Feasibility Study**

by

Keith Sean Cover

B.Sc., The University of Waterloo, 1983

**A Thesis Submitted in Partial Fulfilment of
The Requirements for the Degree of
Master of Science**

in

**The Faculty of Graduate Studies
Department of Geophysics and Astronomy**

We accept this thesis as conforming
to the required standard

The University of British Columbia

October, 1986

© Keith Sean Cover, 1986

In presenting this thesis in partial fulfilment of the requirements for an advanced degree at the University of British Columbia, I agree that the Library shall make it freely available for reference and study. I further agree that permission for extensive copying of this thesis for scholarly purposes may be granted by the head of my department or by his or her representatives. It is understood that copying or publication of this thesis for financial gain shall not be allowed without my written permission.

Department of Geophysics & Astronomy

The University of British Columbia
1956 Main Mall
Vancouver, Canada
V6T 1Y3

Date 86 10 08

Abstract

The fluxgate electric field meter is a new solid-state instrument capable of measuring slowly varying electric fields equally well in an insulating or conducting medium with high resolution. The field meter determines the strength of an electric field by measuring the potential difference between two insulated electrodes immersed in the electric field. The electrode insulation is important because it eliminates the contact potential noise between the conductive material of the electrode and a conductive medium. The capacitance of the insulated electrodes is of the order of 10pF; therefore measurement of the potential difference between the electrodes requires an electrometer with extremely low bias current and high input resistance. A novel electrometer was conceived and designed to accomplish this task. The new electrometer is a solid-state analogue of the vibrating-capacitor electrometer and is claimed to have zero bias current. MOS capacitors are substituted for the vibrating capacitor. The noise level for the crude, proof-of-concept electrometer was $220\mu\text{VHz}^{-1/2}$ at 1Hz. This noise level is only 20 dB worse than the best commercial device I could locate. A crude, proof-of-concept electric field meter constructed with the electrometer had a high frequency cutoff of 150Hz and low frequency cutoff of $100\mu\text{Hz}$. Possible applications of the fluxgate electric field meter include measurement of atmospheric and interplanetary electric fields, measurement of static charge buildup, and geophysical surveys.

Table of Contents

Abstract	ii
Table of Contents	iii
List of Figures	v
Acknowledgements	vi
1. Introduction	1
2. Theory	3
2.1 History	4
2.2 Nonideal Amplifiers	5
3. The Variable-Capacitor Modulator	6
3.1. Equation of the Modulation Circuit	9
3.2. The Fluxgate Mechanism	10
3.3. Electrical Properties of the Sensor	13
4. Realization	17
4.1. The Variable Capacitor	17
4.2. A Nonlinear Capacitor	20
4.3. Feedback Voltage	22
5. Experimental Results	23
5.1. Feedback Linearity	23
5.2. Sensitivity	24
5.3. Directionality of Instrument	25
5.4. Drift Rate	25
5.5. Potential of the Instrument	26
5.6. Instrument Noise	27
6. The Variable-Capacitor Electrometer	27

7. Conclusions	28
Bibliography	30
Appendix A. Electronic Circuitry of the Instrument	65
Appendix B Details of the Variable Capacitor	74

List of Figures

1	Collection capacitor in ambient electric field	32
2	Equivalent circuit of the electric field meter	34
3	Variable-capacitor modulation circuit	36
4	Fluxgate magnetometer operation	38
5	Variable capacitor configuration	41
6	Voltage-versus-capacitance curves for MOSOM capacitors	43
7	Variation of the time varying capacitor's capacitance	45
8	MOSOM nonlinear capacitor design	47
9	MOSOM nonlinear capacitor operation	49
10	Variable-capacitor modulator with feedback	51
11	Feedback Linearity	53
12	Sensitivity-versus-load resistance curve	55
13	Directionality of instrument	57
14	Drift rate	59
15	Potential of the instrument	61
16	A fluxgate electrometer	63
A1	Clock and drive circuit	68
A2	Variable-capacitor modulation circuit	70
A3	Synchronous detector	72

Acknowledgements

I would like to thank John Bennest for his instruction and help with the electronics for the fluxgate electric field meter and for his explanation of the fluxgate magnetometer. To Dr. B. Barry Narod I owe thanks for numerous discussions on the principles and theory of the fluxgate magnetometer and for help with the theory of the fluxgate electric field meter. I would like to thank my supervisor, Dr. R. Don Russell, for pointing out the similarities between the vibrating-capacitor electrometer and the fluxgate electric field meter. I am especially thankful to Dr. Russell for allowing me the freedom and providing the support for me to follow my own ideas. I am also grateful to Dr. L. Young, Dr. P. Janega and Dr. D. L. Pulfrey, all of the Department of Electrical Engineering at the University of British Columbia, for their assistance in the fabrication of the semiconducting wafers used for constructing the fluxgate electric field meter. To D. Schreiber I owe thanks for his help in construction of equipment to test the proof-of-concept electric field meter.

The Natural Sciences and Engineering Research Council of Canada was the primary source of funds for the research on the fluxgate electric field meter under the Operating Grant A0720 and the Strategic Grant G1050. Energy, Mines & Resources Canada, Earth Sciences also assisted under Research Agreement No. 166.

1. Introduction

Of what use is an electric field meter which can measure electric fields equally well in an insulator and a conductor? As Alfvén (1981) pointed out, it is natural to present the results of space exploration with pictures of the magnetic field configuration because magnetic fields are far easier to measure than electric fields. The ease of measurement of magnetic fields in space is primarily due to the ruggedness, small size, low power consumption and high resolution of modern fluxgate magnetometers (Acuna 1974). To be useful for measurements of electric fields in space an electric field meter must have noise level of less than $10\mu\text{Vm}^{-1}\text{Hz}^{-1/2}$ over the frequency bandwidth from 1Hz up to 2MHz (Shawhan *et al* 1981). (Throughout this thesis I will be specifying noise by amplitude spectral density which is covered in many publications including Motchenbacher and Fitchen (1973).) It also must function at frequencies lower than 1Hz but these specifications are not well determined.

Another example of a potentially useful application of an electric field meter is measurement of electric fields in the ocean. The majority of present methods require electric contact with sea water (Filloux 1974). The electrochemical reactions between the sea water and the contacting electrode generate noise which significantly contaminates the signal. Since measurement of electric fields in sea water by an electric field meter would not require electric contact with the sea water, the noise due to contact potential should be eliminated. According to Filloux, the power spectrum, $P(f)$, of the average natural electric activity at the sea floor in the 300nHz to 3mHz band roughly follows the trend $P = k/f$, where f is the frequency in Hertz, and k is $10^{-2}\mu\text{V}^2\text{m}^{-2}$. Present methods using electric contact with sea water require

a separation between electrodes on the order of 100m or more to overcome contact noise and to achieve the desired 1% resolution.

Conventional uses of electric field meters include measuring electric field in clouds (Rust 1978) and measuring electrostatic buildup in locations, such as oil tanker holds and on the surfaces of plastics, to aid in the prevention of explosions and fires (Haenen 1977). Other possible uses of a high resolution wide bandwidth electric field meter include electric field measurement in geophysical surveys such as resistivity, induced polarization and magnetotellurics.

For my M. Sc. thesis in geophysical instrumentation, I conceived, designed, constructed and tested a solid-state fluxgate electric field meter. The instrument consisted of a novel electrometer measuring the potential difference between a pair of insulated electrodes. The prototype was constructed primarily to prove that the concept worked and little effort was made to obtain good specifications in noise or other parameters. None the less, measurements of the noise and other parameters were made to determine a worst case performance of the instrument. The prototype constructed was sensitive to frequencies from 150Hz down to $100\mu\text{Hz}$. The dominant noise source of the electric field meter was the noise of the electrometer. At 1Hz the electrometer had a noise of $220\mu\text{VHz}^{-1/2}$. For the electric field meter prototype the separation between the electrodes was 6.6mm. The resulting noise level of the electric field meter at 1Hz is $33\text{mVHz}^{-1/2}\text{m}^{-1}$. The noise of the electric field meter can be reduced by increasing the separation between the electrodes or reducing the noise of the electrometer.

The instrument is called an "electric field meter" as it can measure slowly varying electric fields equally well in an insulating or conducting medium. The field meter is

referred to as "solid-state" because it has no moving parts. If the fluxgate electric field meter is analysed in a certain way its mechanism for measuring the vector component of an electric field is similar to that used by the fluxgate magnetometer (Primdahl 1979); thus the modifier "fluxgate."

2. Theory

Electric field meters, such as the fluxgate, which are able to measure electric fields with no current flowing along the field lines cannot extract energy from the field to generate a signal and must extract the required energy from another source. Consider two electrodes in an ambient electric field as shown in Figure 1. The two electrodes together form a capacitor which will be called the collection capacitor and has capacitance C_c . The electric field in which the collection capacitor is immersed induces a potential difference, V_c , across the electrodes. Ignoring no edge effects, the value of V_c will be equal to $\mathbf{X} \cdot \mathbf{E}$; where \mathbf{X} and \mathbf{E} are vector quantities. The vector \mathbf{X} has an amplitude that is the distance between the electrodes and a direction that is normal to the surface of the electrodes. The vector \mathbf{E} describes the strength and direction of the ambient electric field.

If an electrometer with zero input bias current and infinite input resistance is connected to the collection capacitor electrodes V_c can be measured accurately. Assuming \mathbf{X} is known, the vector component of \mathbf{E} parallel to \mathbf{X} is calculable. But no one has invented an electrometer with both these ideal characteristics. Finite input resistance and a nonzero input bias current will cause the value of V_c to drift, interfering with the measurement of the ambient electric field. The finite input resistance will dissipate the energy stored in the capacitor until there is zero potential

drop across the capacitor. The energy dissipated by the finite input resistance must somehow be replaced.

2.1. History

Once the collection capacitor has been discharged it must somehow be recycled before it is again possible to measure the electric field. Flipping the capacitor upside down relative to the electric field induces a new potential difference across the electrodes of $-2\mathbf{E} \cdot \mathbf{X}$ and accomplishes the recycling. The effect is the same as if the direction of the electric field had been reversed. The energy the collection capacitor supplies as a charge flow comes from the work done in flipping the electrodes over in the electric field. Russelvedt in 1925 invented a instrument using this principle and called it an arigmeter (Chalmer 1967). An arigmeter has the major disadvantage of requiring a mechanical instrument to flip the electrodes.

Another mechanical method for measuring an electric field without loading the field was described by de Saussure in 1779 (Chalmer 1967). If one of the electrodes of the collection capacitor is moved away from the other along the field lines, a new charge difference is induced between the electrodes which can again be measured by an electrometer. Moving the electrodes back and forth generates a signal proportional to the ambient electric field. The energy to generate the signal comes from the energy supplied to move the electrodes.

Imianitov (1949) suggested a design for a solid-state electric field meter using a ferroelectric material. The suggested field meter, as described by Chalmer (1967), involved using a strong electric field to saturate the dielectric constant of a ferroelectric material. The changing dielectric constant of ferroelectric was intended to modulate the ambient electric field the ferroelectric was immersed in. The modulated ambient

electric field could then be detected with capacitive electrodes. In the early stages of my research into the fluxgate electric field meter, before I had found the suggestion by Imiantov, I conducted experiments with this type of field meter and I obtained no useful results. I can only surmise Imiantov arrived at the same conclusion as I could find no other references to this suggestion.

2.2. Nonideal Amplifiers

Since I was interested in designing a high resolution, rugged, low power electric field meter, I chose to use a solid-state electrometer for the electrometer in Figure 1. Figure 2 shows a more realistic schematic diagram of the electric field meter with additional components that correspond to the nonideal characteristics of the electrometer. The electrometer circuit I selected for the fluxgate electric field meter involves a modification of the circuit in Figure 2; but its nonideal operating characteristics can be handled mathematically in a similar manner. The aim of this section is to determine what specifications of nonideal electrometers a solid-state electric field meter requires for satisfactory performance.

Simple circuit analysis will give the effects of input offset voltage, V_{os} , input bias current, I_b , and finite input impedance of the electrometer on the performance of the electric field meter; therefore only the results will be given. By measuring the performance of the electric field meter it is possible to determine the electrometer's input characteristics. An initial potential difference induced across the collection capacitor will decay exponentially. The time constant of the decay will be $R_{in}C_c$. The output voltage of the electrometer, V_{out} , will approach the value $I_b R_{in} + V_{os}$ at large time. In an ideal world $I_b R_{in} + V_{os}$ would remain constant. Unfortunately, in real electrometers it varies with time by an amount that is a significant part of

its value. This variation is a source of noise. In calculating the relationship between the ambient electric field, E , and V_{out} an ideal electrometer is normally assumed; therefore the ambient electric field is assumed to be related to the output voltage by $-E \cdot X = V_{out}$.

As an example, consider a collection capacitor with an separation, X , of 8mm and a capacitance, C_c , of 15pF. These are the parameters of the collection capacitor used by the prototype. For resolution of the signal in the ocean bottom electric field problem mentioned in the introduction, a low frequency cut off of 300nHz is necessary (Filloux 1974). Treating the circuit formed by the collection capacitor and the input resistance of the electrometer as a simple resistor-capacitor circuit, to achieve the necessary cutoff frequency an input resistance of greater than $4 \times 10^{16} \Omega$ is needed.

The highest input resistance commercial solid-state electrometer that I could find is the Keithly 642. The guarded MOSFET input stage of the 642 has an input resistance of $10^{16} \Omega$ and a noise of $20 \mu V Hz^{-1/2}$ at 1Hz. It also has a input bias current of $5 \times 10^{-17} A$ within the temperature range of 22C to 24C. An amplifier with these specifications would result in an electric field meter, using the above collection capacitor, with a 3 decibel low frequency cutoff of $1 \mu Hz$ and an $I_b R_{in} + V_{os}$ of 500mV. These specifications, while they may be useful for some electric field meter applications, are not good enough for many electric field meter applications. In particular, the large voltage drop across the input resistance due to the bias current will cause serious drift. Also, the limited temperature range of the instrument would cause problems. An electrometer with better specifications is desirable.

3. The Variable-Capacitor Modulator

Figure 3 show a simplified schematic of the modulation part of the electrometer used to measure the voltage across the collection capacitor. The modulation part of the electrometer consists of a time varying capacitor and a load resistor placed in series with the collection capacitor. Strictly speaking, the collection capacitor is not part of the electrometer but is a voltage source. But the electrometer as shown will only function with capacitive voltage sources. Section 6 of this paper will cover the electrometer configuration which will handle noncapacitive sources. An AC amplifier across the load resistor and a synchronous detector fed by the AC amplifier are the two parts of the electrometer not shown in Figure 3. The modulation circuit, including the collection capacitor, will be called the variable-capacitor modulator. The electrometer will be called the fluxgate electrometer or simply the electrometer.

If the capacitance of the time varying capacitor is initially very much smaller than collection capacitor's all the charge will remain on the collection capacitor. But when the time varying capacitor's capacitance approaches the capacitance of the collection capacitor, charge will flow from the collection capacitor through the load resistor and on to the time varying capacitor. The flow of charge through the load resistor will be proportional to the initial voltage cross the collection capacitor. Therefore, by Ohm's Law the voltage drop across the load resistor will be proportional to the initial voltage across the collection capacitor. Varying the capacitance of the time varying capacitor periodically with time will generate a periodic signal across the load resistor. Hence, the amplitude of the periodic signal across the load resistor will be proportional to the initial voltage drop across the collection capacitor.

For the fluxgate electric field meter the time varying capacitor consists of two nonlinear capacitors. At this point it is useful to outline the definitions I will use to describe linear and nonlinear capacitances. The definitions I have chosen are those used by Löcherer and Brandt (1982). A capacitor is linear if it obeys the relationship $VC = q$; where V is the voltage across the capacitor, q is the charge stored in the capacitor and C is the capacitance of the capacitor and is independent of the value of V . A nonlinear capacitor is a capacitor which does not have a linear relationship between charge and voltage. The definition of the capacitance of a nonlinear capacitor is ambiguous. In this thesis I will use the differential definition of capacitance. By this definition the capacitance is defined as $C(V) = (dq / dv)_{v=V}$.

The node between the collection and time varying capacitor is only capacitively coupled to the rest of the circuit; therefore conservation of charge dictates that the charge on the collection capacitor when the capacitance of the time varying capacitor is very small must be equal to the sum, at any time, of the charge on the collection and variable capacitors. For convenience, this sum of charges will be called the induced charge. A leakage path for electrons from the node between the collection and variable capacitors will allow the induced charge to leak away and cause a signal drift. The resistance the collection and variable capacitors must be very large to keep the leakage of the induced charge very small.

The variable-capacitor modulator is almost identical to that of the vibrating-capacitor electrometer (Palevsky *et al* 1947); but, there are two important differences. One difference is that the variable-capacitor electrometer uses a solid-state modulator while the vibrating-capacitor electrometer uses a mechanical one. Solid-state modulation has the advantages, among others, of needing less power, of being more rugged and of supporting modulation to a higher frequency. A solid-state modulator should

be capable of modulation at the megahertz range. The prototype electric field meter constructed uses a carrier of 32 KHz . High modulation frequency is valuable because the power generated by the variable-capacitor modulation circuit increases with increased carrier frequency. The extra power will reduced the effect of the thermal noise of the load resistor as well as most other noise sources in the circuit.

The second important difference between the modulator used in the vibrating-capacitor electrometer and the variable-capacitor modulator is the way in which the charge is delivered to the collection capacitor. In the vibrating-capacitor electrometer the charge is delivered via a high resistance resistor to the node between the variable and collection capacitors (Palevsky *et al* 1947). The end of the high resistance resistor not attached to the node between the variable and collection capacitors is attached to the voltage source of which we are interested in measuring the potential. This configuration will be covered in more detail in Section 6 on the fluxgate electrometer. In contrast, the fluxgate electric field meter has its charged induced on the collection capacitor by the potential difference induced between the collection capacitor electrodes by the ambient electric field.

3.1. Equation of the Modulation Circuit

The differential equation describing the variable capacitor modulator follows easily by application of Thévenin's theorem and Kirchhoff's Law (Millman and Halkias 1967). Besides the collection capacitor, C_c , the variable capacitor, $C_v(t)$, the load resistance, R , and the potential drop across the unloaded collection capacitor due to the ambient electric field, V_e , the other required parameters are the charges on the collection and variable capacitors, q_c and q_v respectively. Thévenin's theorem allows V_e to be placed in series with the collection capacitor to represent the effect

of the ambient electric field. The induced charge is accounted for by the V_e term; therefore, since charge must be conserved, the charge on the collection and variable capacitors must be equal. In other words $q_v = q_c$. Applying Kirchhoff's law to Figure 3, taking into account Thévenin's theorem, gives the equation

$$R\dot{q}_v + q_v \left(\frac{1}{C_c} + \frac{1}{C_v(t)} \right) = V_e. \quad (1)$$

Equation (1) can be simplified slightly by the change of variables

$$C_s(t) = \frac{C_v(t)C_c}{C_v(t) + C_c} \quad (2)$$

yielding

$$R\dot{q}_v + \frac{q_v}{C_s(t)} = V_e. \quad (3)$$

The mathematical difficulty in solving equation (3) depends on the choice of function $C_s(t)$.

Up to this point it as be assumed that the only source of charge has been the induced charge caused by the ambient electric field. If there is a charge on the collection or variable capacitor when the ambient electric field is zero it will show up in the electric field measurement as an apparent electric field offset. The additional charge could be due to static charge buildup or some other cause. With time, the additional charge will drain off through the leakage resistance and contribute to the drift of the electric field meter.

3.2. The Fluxgate Mechanism

You may be wondering why I chose to call this instrument a “fluxgate” electric field meter. The reason is that the electric field meter’s method of modulating the ambient electric field developed from the fluxgate magnetometer. To understand this analogy it is useful to understand how the fluxgate magnetometer senses magnetic fields.

The object of magnetic fluxgating is to make a slowly varying magnetic field measurable without mechanical motion of a sense coil. Primdahl (1979) gives a brief description of the method. It was explained to me in more detail by John Bennest, a technician in my lab. By Faraday’s law, inducing an electromotive force in a conductor requires relative motion between the conductor and the ambient magnetic field. Since the sense coil must remain stationary, the ambient magnetic field must change to induce a signal in the sense coil. The change in the magnetic field is accomplished by modulating the permeability of a ferromagnetic core. The modulated permeability in turn distorts the magnetic field lines near the core. Figures 4(a) and 4(b) are diagrams of the field line distortions. The time varying distortion of the field lines induces a signal in the sense coil. The induced signal will show up as a voltage drop across the load resistor which in turn can be measured.

The equation describing the resistively loaded fluxgate magnetometer is an analogue of the equation for the fluxgate electrometer given in equation (3). Russell *et al* (1983) gave the equation describing the fluxgate magnetometer as

$$\dot{\phi} + \frac{R\phi}{L(t)} = \frac{l}{n} \frac{d}{dt} (HL(t)); \quad (4)$$

where ϕ is the magnetic flux in the sense coil, l/n is a geometric constant of the sense coil, R is the load resistor across the sense coil and $L(t)$ is the time varying inductance of the sense coil. The inductance of the sense coil is time varying because of the time varying permeability of the ferromagnetic core. It is useful to remember that magnetic flux, ϕ , is equal to $L(t)i$; where i is the current through the sense coil. When the inductance of the sense coil changes the flux is conserved. In the fluxgate electric field meter when the capacitance of the variable capacitor changes conservation of charge applies. Therefore, the flux of the fluxgate magnetometer is analogous to the charge of fluxgate electric field meter.

The method normally used in the fluxgate magnetometer for modulating the ferromagnetic core is straight forward. A second coil is placed around the ferromagnetic material of the core. This second coil is referred to as the drive coil. The drive coil is used to generate a periodic very intense magnetic field which saturates the ferromagnetic core thus modulating the permeability. The drive and sense coil are usually positioned relative to each other so their mutual inductance is small. The small mutual inductance prevents the very intense field from the drive coil from dominating the signal in the sense coil caused by the ambient magnetic field.

The fluxgate electric field meter measures a slowly varying ambient electric field in the same way as the fluxgate magnetometer measures a slowly varying ambient magnetic field— by modulating it. The modulation is accomplished by the time varying capacitor. The time varying capacitor forces the induced charge to move back and forth between the variable and collection capacitors. The motion of the induced charge generates a time varying electric field around the collection capacitor electrodes. Instead of measuring the modulated electric field with a second set of electrodes, I have chosen to measure the rate of charge flow from the variable to

collection capacitors which is also proportional to the ambient electric field. Measuring the rate of charge flow between the variable and collection capacitors makes the fluxgate electric field meter easier to construct.

3.3. Electrical Properties of the Sensor

The important properties of any electrical sensor are sensitivity, impedance, upper and lower limits on bandwidth, and noise level. The lower limit on bandwidth is determined by drift and noise. Sensor drift was covered during the treatment of nonideal electrometers earlier in this thesis. The prediction of the noise level is difficult at best and will not be a concern of this thesis. But the sensitivity, impedance and upper limit of the bandwidth follow from the solution of equation (3). Choosing

$$C_s(t) = \begin{cases} C_1 & \text{for } nt_p \leq t < nt_p + t_1; \\ C_2 & \text{for } nt_p + t_1 \leq t < (n+1)t_p; \end{cases} \quad n = 0, 1, 2, \dots \quad (5)$$

allows for a closed-form solution of equation (3); where t_p is the period of one complete cycle and t_1 is the time after the starting transition of a cycle at which the second transition occurs. Equation (3), using the time varying capacitance given in equation (5), is also easy to implement with electrical circuitry to a good approximation.

An upper limit on the bandwidth follows from the homogeneous solution to equation (1), denoted $q_v^h(t)$. A method of finding the homogeneous response of linear differential equations with periodic coefficients was first published by Floquet (1883); a modern reference is Nayfeh and Mook (1979). Russell *et al* (1983) applied the technique to the fluxgate magnetometer. Floquet showed the homogeneous solution has the form of a periodic function times an exponential decay. The time constant of the

exponential decay determines the transient response time and thus the upper limit on bandwidth of the variable-capacitor modulation circuit. Using the time varying capacitance described in equation (5), the form of the homogeneous solution depends upon the fact that if $q_v^h(t)$ is a solution to equation (3) then so must $q_v^h(t + t_p)$ due to periodicity and linearity; therefore, the ratio $q_v^h(t) / q_v^h(t + t_p)$ is a constant and hence, the transient response time, γ , is

$$\gamma = \frac{-t_p}{\ln [q_v^h(t_p)/q_v^h(0)]}. \quad (6)$$

The upper limit on the bandwidth is then $1/(2\pi\gamma)$.

Calculating $q_v^h(t_p)/q_v^h(0)$ is straightforward for the $C_s(t)$ function given in equation (5). The discontinuities in $C_s(t)$ break equation (3) into 2 separate equations which apply during alternate time periods. The conservation of charge is the continuity condition.

The two parts of equation (3) yield the homogenous solutions

$$\begin{aligned} q_1^h(t) &= A_n e^{-t/(RC_1)} \text{ for } nt_p \leq t < nt_p + t_1; \\ q_2^h(t) &= B_n e^{-t/(RC_2)} \text{ for } nt_p + t_1 \leq t < (n+1)t_p. \end{aligned} \quad n = 0, 1, 2 \dots \quad (7)$$

The continuity conditions at the transition points are given by conservation of charge, thereby giving the value of the coefficients, A_n and B_n . The only exception is A_0 which is determined by the initial condition $q_v(0)$. Solving equation (7) for

$q_v^h(t_p)/q_v^h(0)$ produces

$$\frac{q_v^h(t_p)}{q_v^h(0)} = \exp \left[- \left(\frac{t_1}{RC_1} + \frac{t_p - t_1}{RC_2} \right) \right]. \quad (8)$$

Substituting into equation (6) yields

$$\gamma = \frac{t_p}{\left(\frac{t_1}{RC_1} + \frac{t_p - t_1}{RC_2} \right)}, \quad (9)$$

the transient response time, which leads directly to the upper limit on the bandwidth.

Before it is possible to calculate the sensitivity of the fluxgate electric field meter, it is necessary to define the sensitivity. In this thesis I will define the sensitivity, S , of the fluxgate electric field meter to be the root-mean-square average of the modulation frequency voltage across the load resistor at divided by the strength of the electric field normal to the collection capacitor electrodes. The root-mean-square average of the modulation frequency voltage across the load resistor will be called the "second harmonic voltage." The second harmonic voltage is noted by the symbol V_{2nd} . The reason for the modifier "second harmonic" will become clear later in this thesis. This definition of sensitivity ties together well with the definition of "conversion efficiency" defined by Palevsky *et al* (1947) for the vibrating-capacitor electrometer. They defined conversion efficiency, α , as V_{2nd} divided by the input voltage. The corresponding definition for the fluxgate electric field meter would be $\alpha = V_{2nd}/V_e$; where V_e is the potential drop across the unload collection capacitor due to the ambient electric field. Thus, the sensitivity and the conversion efficiency are related by the equation $S = \alpha X$; where X is the amplitude of the vector \mathbf{X} . Because \mathbf{X}

is a measure of the separation between the collection capacitor electrodes and can easily be measured only a method to calculate the conversion efficiency is needed.

Calculation of the conversion efficiency of the field meter involves calculating the steady-state solution of equation (3). A method of finding a steady-state solution, for this type of problem, was presented by Narod and Russell (1984). To obtain the steady-state solution, one needs the particular solution to equation (3) (Boyce and DiPrima 1977). Equation (3), using the function for $C_v(t)$ defined in equation (5), yields the two-part particular solution

$$\begin{aligned} q_1^p(t) &= V_e C_1 \text{ for } nt_p \leq t < nt_p + t_1; \\ q_2^p(t) &= V_e C_2 \text{ for } nt_p + t_1 \leq t < (n+1)t_p. \end{aligned} \quad n = 0, 1, 2 \dots \quad (10)$$

Adding the homogeneous and particular solutions gives the two-part complementary solution

$$\begin{aligned} q_{b1}^c(t) &= A_n e^{\frac{-t}{RC_1}} + C_1 V_e \text{ for } nt_p \leq t < nt_p + t_1; \\ q_{b2}^c(t) &= B_n e^{\frac{-t}{RC_2}} + C_2 V_e \text{ for } nt_p + t_1 \leq t < (n+1)t_p. \end{aligned} \quad n = 0, 1, 2 \dots \quad (11)$$

By definition, the steady-state solution has the property

$$q_v^s(0) = q_v^s(t_p). \quad (12)$$

Combining the two parts of equation (10) with equation (11) and using conservation of charge as the continuity condition yields the initial condition for the steady-state

solution

$$q_v^s(0) = \frac{C_1 V_e \exp \left[- \left(\frac{t_1}{RC_1} + \frac{t_p - t_1}{RC_2} \right) \right] + (C_1 - C_2) V_e \exp \left[\frac{(t_p - t_1)}{RC_2} \right] + C_2 V_e}{1 - \exp \left[- \left(\frac{t_1}{RC_1} + \frac{t_p - t_1}{RC_2} \right) \right]}. \quad (13)$$

The initial condition imposed upon the complementary solution gives the periodic current waveform generated by the modulation circuit. Once one has the periodic current waveform a simple application of Ohm's Law will give the periodic voltage waveform across the load resistor. A Fourier series decomposition of the voltage waveform, with some additional manipulation, will yield V_{2nd} .

Knowing the output impedance of the variable capacitor modulator is important because a high output impedance causes high noise in the input stage of the AC amplifier. Millman and Halkias (1967) define the output impedance at the second harmonic, r_p , to be

$$r_p = \left(\frac{\partial V_{2nd}}{\partial I} \right); \quad (14)$$

where I is the current drawn by the input stage, V_{2nd} is the voltage across the input stage. The field effect transistor input stage of the can be modelled mathematically by a resistance of $10^{12} \Omega$. Combining the parallel resistance of the input stage and the load resistor gives a new resistance which can be treated mathematically as load resistance without an amplifier across it. Using the procedure previously described it is possible to calculate V_{2nd} at any desired load resistance and since the two parallel resistors can be treated as one it is also possible to calculate I . Therefore the derivative in equation (14), the output impedance, can be calculated.

4. Realization

4.1. The Variable Capacitor

There is one major stumbling block to the design of the fluxgate electric field meter. It is finding a solid-state variable capacitor. The variable capacitor must have an extremely high resistance to prevent charge induced by the ambient electric field from leaking from one side of the collection capacitor to the other. It should be able to vary repeatably its capacitance down to about 10pF to keep the associated electronics simple. It is convenient, from a design point of view, to use a voltage to control the variable capacitor.

Abe *et al* (1971) used a novel configuration for the variable capacitor. Figure 5 shows the circuit for the Abe *et al* (1971) variable capacitor using two nonlinear capacitors and a differential drive symmetric about ground. The two nonlinear capacitors should be well matched with voltage-versus-capacitance curves symmetric about zero voltage. If the two nonlinear capacitors are perfectly matched and have perfectly symmetric voltage-versus-capacitance curves, the potential of the output node, the node where the two nonlinear capacitors join, will remain exactly at ground. At the same time the capacitance to ground of the output node varies at twice the frequency of the differential drive frequency. For the remainder of the thesis the frequency of the differential drive will be called the “fundamental frequency” and the frequency of the variable capacitor will be referred to as the “second harmonic frequency.”

Figure 6 shows the curve depicting voltage versus capacitance curve for each of the two nonlinear capacitors used in testing the fluxgate electric field meter. The two nonlinear capacitors are imperfectly matched. If the two nonlinear capacitors are not perfectly matched or the differential drive is not perfectly balanced the output

node will not, in general, be held at ground. The imperfections will produce an additional signal across the load resistor usually at both the fundamental and second harmonic frequencies. If the additional signal were to remain constant with time it could, in principle, be subtracted. But, due to drifts of components with time and temperature, this additional signal drifts and leads to additional noise.

Imperfect matching of the two nonlinear capacitors also leads to another somewhat unexpected occurrence. Consider the situation where the capacitance of each of two nonlinear capacitors is maximum with zero voltage across each capacitor and decreases with increasing voltage. This is the case for the two nonlinear capacitors used in the prototype. When a voltage is applied across the two nonlinear capacitors in series there will be a greater voltage drop across the capacitor with the smaller capacitance. This in turn will decrease the capacitance of the smaller capacitor. The smaller capacitor will again have a larger voltage drop across it. This cycle will continue until a stable point is reached. A stable point does exist because the total potential drop across the variable capacitors is finite and the potential at the point between the two nonlinear capacitors must be between the potentials at either end of the two nonlinear capacitors.

Figure 7 shows the estimated capacitance of the unloaded output node of the variable capacitor with respect to ground as a function of time. The method of estimating the capacitance-versus-time curve drew upon the two capacitance curves displayed in Figure 6 and the differential drive voltages shown in Figure 7 to numerically simulate the variable capacitor circuit in Figure 5.

The nonlinear nature of the variable capacitor draws into question whether it is best to solve the variable capacitor as an isolated problem and then substitute the

generated capacitance-versus-time curve into equation (3). The loading of the variable capacitor by the collection capacitor and load resistor may change the capacitance-versus-time curve. A more accurate modelling of the variable-capacitor modulation circuit might be achieved by numerically modelling the circuit as a whole as opposed to modelling it in sections; but, for simplicity I will break the modulation circuit into sections for the duration of this thesis.

4.2. A Nonlinear Capacitor

Possible candidates for nonlinear capacitors included ferroelectric capacitors, reversed bias diodes, and metal-oxide-silicon capacitors. Metal-oxide-silicon capacitors are normally called MOS capacitors. Ferroelectric capacitors are difficult to fabricate and require a very high voltage to drive them into their nonlinear range. Abe *et al* used ferroelectric capacitors for their nonlinear capacitors. Reversed bias diodes are unsuitable because of their high leakage current. The leakage currents are typically on the order of $1\mu\text{A}$ and it is difficult to make them much smaller without cryogenic cooling. I chose MOS capacitors for use in the prototype of the electric field meter for a number of reasons including their extremely high resistance and relative ease of fabrication. Sze (1981) mentions the use of MOS capacitors in a semipermanent computer memory called EPROM. EPROM memory uses MOS capacitors only a fraction of a picofarad in size to hold a significant charge as long as 100 years. This implies a resistance on the order of $10^{21}\Omega$. Properties of MOS capacitors are covered in detail by Grove (1967) and by Nicollian and Brews (1982).

The voltage-versus-capacitance curve of a MOS capacitor is not symmetric but it is possible to fabricate a capacitor with a symmetric voltageversuscapacitance curve by placing two MOS capacitors back-to-back as shown in Figure 8. Löcherer and

Brandt (1982) mention this configuration and give it an appropriate name. A MOS capacitor is a special type of MIS capacitor; where MIS is a acronym for metal-insulator-silicon. Löcherer and Brandt (1982) called the capacitor formed by two back-to-back MIS capacitors a MISIM capacitor. By analogy I will call the capacitor formed by two backto back MOS capacitors a MOSOM capacitor. The voltage-versus-capacitance of a MOSOM capacitor will be approximately symmetric. For the sake of completeness I will give a rough explanation of the principles of the MOSOM capacitor.

Although either N-type or P-type silicon is suitable for the fabrication of the MOSOM capacitors, N-type silicon was used for testing the prototype. At room temperature, under no electric field, the silicon is conductive due to the thermally generated electrons; but the highly resistive layer of silicon dioxide makes the wafer, as a whole, a capacitor with all the voltage drop across the insulating oxide layer.

The sudden application of a potential difference between the two areas of metalization will drive all of the electrons near the negative plate away from the negative plate as shown in Figure 9(a). This leaves a region of the silicon near the negative plate depleted of free charge carriers and effectively an insulator. This additional layer of insulating material decreases the capacitance of the MOSOM capacitor. If the direction of the intense electric field is quickly reversed, a new depletion zone is created adjacent to the second charged plate and the original depletion zone is returned to a conducting state, as shown in Figure 9(c).

The exact switching time of a MOSOM capacitor depends upon the particular details of fabrication; but the switching time should be about the same as variable

capacitor diodes which also use a depletion zone to vary capacitance. The switching time of variable capacitance diodes is in the range 10^{-10} to 10^{-13} seconds.

4.3. Feedback Voltage

One problem with the variable-capacitor modulator using voltage dependent capacitors is that the ambient electric field, if it is intense enough, may interfere with the differential drive voltage changing the capacitance-versus-time waveform. This would lead to a nonlinear variable-capacitor modulator. In addition, any drift in the values of the components in the modulation circuit due to time or temperature change will also affect the linearity of the instrument. As with many instruments with a nonlinear response, a good solution is the use of feedback.

In the mathematical analysis of the modulation circuit, the voltage source due to the ambient electric field across the collection capacitor was represented by the voltage source V_e . A feedback voltage source, denoted V_f , can be inserted into the modulation circuit as shown in Figure 10. The two voltage sources V_f and V_e will add to produce a net voltage source for the modulation circuit; therefore, V_f can be used as a feedback voltage to cancel V_e .

Ideally, the feedback voltage source would float independent of ground; but in practice the feedback voltage source will be tied to ground via a relatively low resistance path. Positioning of the feedback voltage source in the variable-capacitor modulation circuit is therefore crucial to prevent the feedback voltage source from drastically reducing the input resistance on the variable-capacitor modulation circuit. Figure 10 shows the the feedback voltage source in it correct position adjacent to ground. By placing the feedback back voltage source adjacent to ground the problem of the low resistance path to ground is eliminated.

A feedback loop configuration was not used in the prototype because the aim of the prototype was to test the open loop characteristics of the fluxgate electric field meter; but feedback as a method of generating a signal was tested and shown to perform as predicted.

5. Experimental Results

Extensive measurements of the specifications of the prototype fluxgate electric field meter were carried out. The prototype instrument used the MOSOM capacitors, described earlier, for the nonlinear capacitors in the variable-capacitor modulator. The collection capacitor had a separation between conducting electrodes of 8mm and a capacitance, C_c , measured to be 15pF. The area of the collection capacitor electrodes was 100mm^2 each. The collection capacitor electrodes were insulated from each other by air. The load resistance used in the variable-capacitor circuit was $1M\Omega$ unless otherwise stated. A pair of 2m by 3m conducting plates separated by 1m sourced the ambient electric field used to test the prototype. The 2m by 3m plates will be called source plates. The prototype was suspended between the source plates.

5.1. Feedback Linearity

The feedback voltage and the ambient electric field across the collection capacitor add to give the total voltage which determines the amplitude of the second harmonic frequency. By ensuring that the ambient electric field across the collection capacitor is zero it is possible to vary the feedback voltage and determine the relation between the feedback voltage and the second harmonic voltage. Figure 11 displays the measured relationship. The full range of measure of the feedback voltage was swept in one

second during the execution of the measurement. In Figure 11 the slope of the line, which corresponds to the conversion efficiency, is 0.10.

If the feedback voltage is kept at ground the second harmonic voltage will be determined by the ambient electric field across the collection capacitor. To make future results of measurements on the electrometer more understandable, all output voltages from the fluxgate electric field meter will be quoted in terms of "equivalent feedback voltage." The equivalent feedback voltage is the feedback voltage which must be applied, when there is no ambient electric field across the collection capacitor, which will generate the equivalent second harmonic output voltage.

5.2. Sensitivity

The theory of the electric field meter presented predicts the electric field meter sensitivity will vary with load resistance. Figure 12 is a graph of conversion efficiency versus load resistance. As mentioned earlier, the conversion efficiency is directly proportional to the sensitivity. The small circles of Figure 12 represent the measured data points. The solid line depicts the predicted conversion efficiency using the formulas developed previously. The parameters used for the predicted conversion efficiency are those of the capacitance-versus-time curve shown in Figure 7. They are a second harmonic frequency of 31 250 Hz , and a time varying capacitor which spends 25% of the time at 33pF and the other 75% of the time at 17pF.

The match between the measured and predicted conversion efficiencies is poor. This discrepancy could be explained by an inaccurate voltage-versus-capacitance curve for the time varying capacitor. It also may be due to an undetected phase shift in the synchronous detector circuitry. An undetected phase shift could change

the apparent sensitivity because the synchronous detector is phase sensitive. More measurements are required before the exact explanation is known.

5.3. Directionality of Instrument

The directionality of the fluxgate electric field was measured by rotating the instrument in a 1 Vm^{-1} electric field and measuring the equivalent feedback voltage as a function of direction relative to the electric field. The results of the measurement, with an offset voltage subtracted to improve the symmetry about zero volts, are displayed in Figure 13. It shows good directionality. The measured data gave a separation between the collection capacitor electrodes of 6.6mm. The separation between the collection capacitor electrodes, measured with a ruler, was 8mm. The agreement between these two values is reasonable.

5.4. Drift Rate

To measure the drift rate of the electric field meter I placed a charge on the collection capacitor and monitored the output voltage of the field meter. Figure 14 shows the results. The decay can be divided up roughly into four sections each section appearing to have its own characteristics. The first section, from 0.0Ks to 0.5Ks, is probably noise generated by motion of people around the electric field meter.

The second section, from 0.5Ks to about 2Ks, appears to be a linear decay. The linear decay of the voltage could be due to a current limited conduction path either between the electrodes of the collection capacitor or through some other leak path.

The third section, roughly from 2Ks to 8Ks, appear to be an exponential decay with a time constant of approximately 2Ks. If we assuming the exponential decay is caused by the 15pF collection capacitor discharging through a leakage path the time constant of the exponential decay gives the resistance of the leakage path to be about

$10^{14}\Omega$. The resistance of the leakage path corresponds to the input resistance. The route of the leakage path is unknown. Conduction through the air between electrodes of the collection capacitor is one possible path. A leakage path between the two areas of metalization of one of the MOSOM capacitors is another possibility.

According to Volland (1982), the resistivity of dry air at sea level is approximately $10^{14}\Omega m$; although the resistivity value can vary by at least a factor of three due to humidity and air pollutants. The air gap between the two electrodes of the collection capacitor had a width of 8mm and an area of $0.01m^2$. Assuming resistivity for air of about $10^{14}\Omega m$, the leakage resistance of the collection capacitor due to air would be about $8 \times 10^{13}\Omega$. This value agrees well with the measured leakage resistance.

The fourth section of the decay curve is the flat section after 10Ks. The section corresponds to an offset voltage with a value of -159mV. In the unlikely case that the offset voltage is solely due to an input bias current then the input bias current would be about 1fA. The more probable case of the offset voltage is the mismatch between the two nonlinear capacitors. If this is the main cause of the offset voltage the input bias current is much less than 1fA. The input bias current is believed to be zero for the fluxgate electrometer.

5.5. Potential of the Instrument

Until now I have only considered the effects of the gradient of the electric potential, the electric field, on the collection capacitor. The total electric potential also has an effect. To measure this effect I applied zero electric field and varied the potential of the electric field meter relative to circuit ground. The potential of the instrument was varied by electrically shorting together the source plates which were previously used to generate the ambient electric field and then varying the potential

of the plates. Figure 15 shows the outcome of the experiment. The slope of the solid line which fits the data is 0.114.

The sensitivity of the fluxgate electric field meter to its own potential as well as the electric field is related to the grounding of the instrument. One electrode of the collection capacitor is DC coupled directly to the same ground as the source plates and is, thus, held solidly at ground potential. The other electrode of the collection capacitor is only capacitively coupled to ground and can "float." The collection capacitor electrode held at ground disturbs the constant potential environment generated by the two source plates. The disturbed field near the grounded collection capacitor electrode changes the potential of the floating electrode of the collection capacitor and induces a charge on the collection capacitor.

It is possible not to have a common ground for the collection capacitor and the source plates. The two circuits would then float in an unpredictable manner and generate a large amount of noise in the signal. It is preferable to have a common ground where the effect of the potential of the sensor is predictable and can be allowed for.

5.6. Instrument Noise

The noise of the prototype fluxgate electric field meter was found to be $220\mu\text{VHz}^{-1/2}$ at 1Hz. The cause of the noise was not seriously investigated because it is considered outside the scope of this thesis. The noise of the lowest bias current commercially available electrometer I could locate, the Keithly 642, (Keithly 1985) is only 20dB better than the crude prototype of the fluxgate electrometer. The crude prototype of the fluxgate electric field meter is about 55 dB noisier than silver-silver chloride electrodes mentioned in the introduction.

6. The Fluxgate Electrometer

The vibrating-capacitor electrometer described by Palevsky *et al* (1947) and the ferroelectric electrometer described by Abe *et al* (1971) are electrometers which can handle noncapacitive voltage sources. The fluxgate electrometer can be configured to accomplish the same task. Figure 16 shows the circuit topography of the modified modulation stage. The collection capacitor is shielded from any external electric field. The potential drop across the collection capacitor is supplied instead via a very high resistance resistor, R_s . The source of the potential is the voltage source, V . R_s must be very large to keep the voltage source from significantly loading the modulation circuit. The resistance of R_s must be very much greater than the inverse of the product of second harmonic frequency and the maximum input capacitance per cycle.

Using a fluxgate electrometer designed to handle non capacitive voltage sources, it is possible to design an electric field meter. The circuit used is the circuit shown in Figure 2. There are two major advantages to this new configuration. Firstly, since the collection capacitor in the modulation stage on the fluxgate electrometer is shielded, it is less prone to having its capacitance altered by nearby conductive materials. Changing the collection capacitor's capacitance will change the conversion efficiency of the modulation circuit. The second major advantage is modularity of the design. It is possible to design and test the fluxgate electrometer independent of the voltage source.

7. Conclusions

The fluxgate electric field meter may have the capability to accomplish the tasks mentioned in the introduction. These tasks included measurement of interplanetary

and ocean bottom electric fields as well as exploration geophysics surveys. The combination of small size, low power consumption and high resolution of the fluxgate electric field meter makes it a very useful instrument. The simple and reasonably accurate theory describing the fluxgate electric field meter will simplify design and construction. The one exception to the accuracy of the theory is the prediction of the conversion efficiency. The theoretical predictions disagrees with experiment results by at least a factor of two. More work is required in this area to determine the cause of the inconsistency.

The theory and concepts of the fluxgate electric field meter drew heavily upon the theory and concepts of the fluxgate magnetometer. A trick used in the fluxgate magnetometer might also be successfully applied to the fluxgate electric field meter. The trick is to parametrically pump the field meter by inductively loading the fluxgate modulation circuit and thus use the time varying capacitance to supply additional amplification. Another possibility, not readily available to the fluxgate magnetometer, is increasing the drive frequency of the fluxgate electrometer into the megahertz range while maintaining the same signal bandwidth. The increased power produced by the modulation circuit at the higher frequency can be used to overcome input noise of the electric field meter's second harmonic amplifier.

In conclusion, I believe that the fluxgate electric field meter is a instrument that has a promising future because of its possible use in a wide range of applications. There are patent applications being pursued in both Canada and in the United States with regards to the fluxgate electric field meter.

Bibliography

Abe Z., Kato Y. and Furuhashi Y. 1971, "A New Second Harmonic Type Ferroelectric Modulator for Electrometer," *Rev. Sci. Instrum.*, **42**, 805-809.

Acuña M. H. 1974, "Fluxgate magnetometers for outer planets exploration," *IEEE Trans. Mag.*, **MAG-10**, 519-23.

Alfvén H. 1981, *Cosmic. Plasma* (Boston: D. Reidel), p 164.

Boyce W. E. and DiPrima R. C. 1977, *Elementary Differential Equations and Boundary Value Problems* (New York: John Wiley & Sons), p 652.

Chalmers J. A. 1967, *Atmospheric Electricity 2nd ed.*, (Toronto: Pergamon Press), p 515.

Filloux J. H. 1974, "Electric Field Recording on the Sea Floor with Short Span Instruments," *J. Geomag. Geoelectr.*, **26**, 269-79.

Floquet M. G. 1883, "Sur les équations différentielles linéaires à coefficients périodiques," *Ecole Normale Supérieure de Paris, Annales Scientifiques 2nd Series*, **12**, 47-88.

Grove A. S. 1967, *Physics and technology of semiconductor devices* (New York: John Wiley & Sons), p 366.

Haenen H. T. M. 1977, "Potential probe measurement analysis and charge distribution determination," *J. of Electrostatics*, **2**, 203-22.

Imianitov I. M. 1949, *Avtorskoe svidetelstvo*, No. 86672, [5.33]

Keithly Instruments Inc. 1985, *1985-1986 Catalog and Buyer's Guide: Electronic Measurement Instruments*, p 99.

Löcherer K-H. and Brandt C-D. 1982, *Parametric Electronics* (Springer-Verlag: New York), p 328.

Millman J. and Halkias C. C. 1967, *Electronic Devices and Circuits* (McGraw-Hill: Toronto), p 752.

Motchenbacher C. D. and Fitchen F. C. 1973, *Low-noise Electronic Design* (New York: Wiley), p 328.

Narod B. B. and Russell R. D. 1984, "Steady-state Characteristics of the Capacitively Loaded Flux Gate Sensor," *IEEE Trans. on Mag.*, **MAG-20**, 592-97.

Nayfeh A. H. and Mook D. T. 1979, *Nonlinear Oscillations* (New York:Wiley), p 704.

Nicollian E. H. and Brews J. R. 1982, *MOS Physics and Technology* (New York: Wiley), p 906.

Palevsky H., Swank R. K. and Grenchik R. 1947, "Design of Dynamic Condenser Electrometers," *Rev. Sci. Instrum.*, **18**, 298-314.

Primdahl F. 1979, "The fluxgate magnetometer," *J. Phys. E: Sci. Instrum.*, **12**, 241-53.

Russell R. D., Narod B. B. and Kollar F. 1983, "Characteristics of the Capacitively Loaded Flux Gate Sensor," *IEEE Trans. on Mag.*, **MAG-19**, 126-30.

Rust W. D. 1978, "A Review of recently developed instrumentation to measure electric fields inside clouds," *Atmospheric Technology*, **8**, 57-65.

Shawhan S. D., Gurnett D. A., Odem D. L., Helliwell R. A. and Park C. G. 1981, "The Plasma Wave and Quasi-Static Electric Field Instrument (PWI) for Dynamics Explorer-A," *Space Sci. Instrum.*, **5**, 535-50.

Sze S. M. 1981, *Physics of Semiconductor Devices 2nd ed.* (John Wiley & Sons: Toronto), p 868.

Volland H. Ed. 1982, *CRC Handbook of Atmospheric Vol. I* (CRC: Boca Rotan), p 377.

Figure 1 Collection capacitor in ambient electric field. A potential difference is induced across the electrodes of the collection capacitor by the ambient electric field. The potential difference is proportional to the strength of the field normal to the electrodes. An ideal electrometer, with infinite input resistance, placed across the collection capacitor would be able to measure the potential difference and thus determine the strength of the field normal the electrodes.

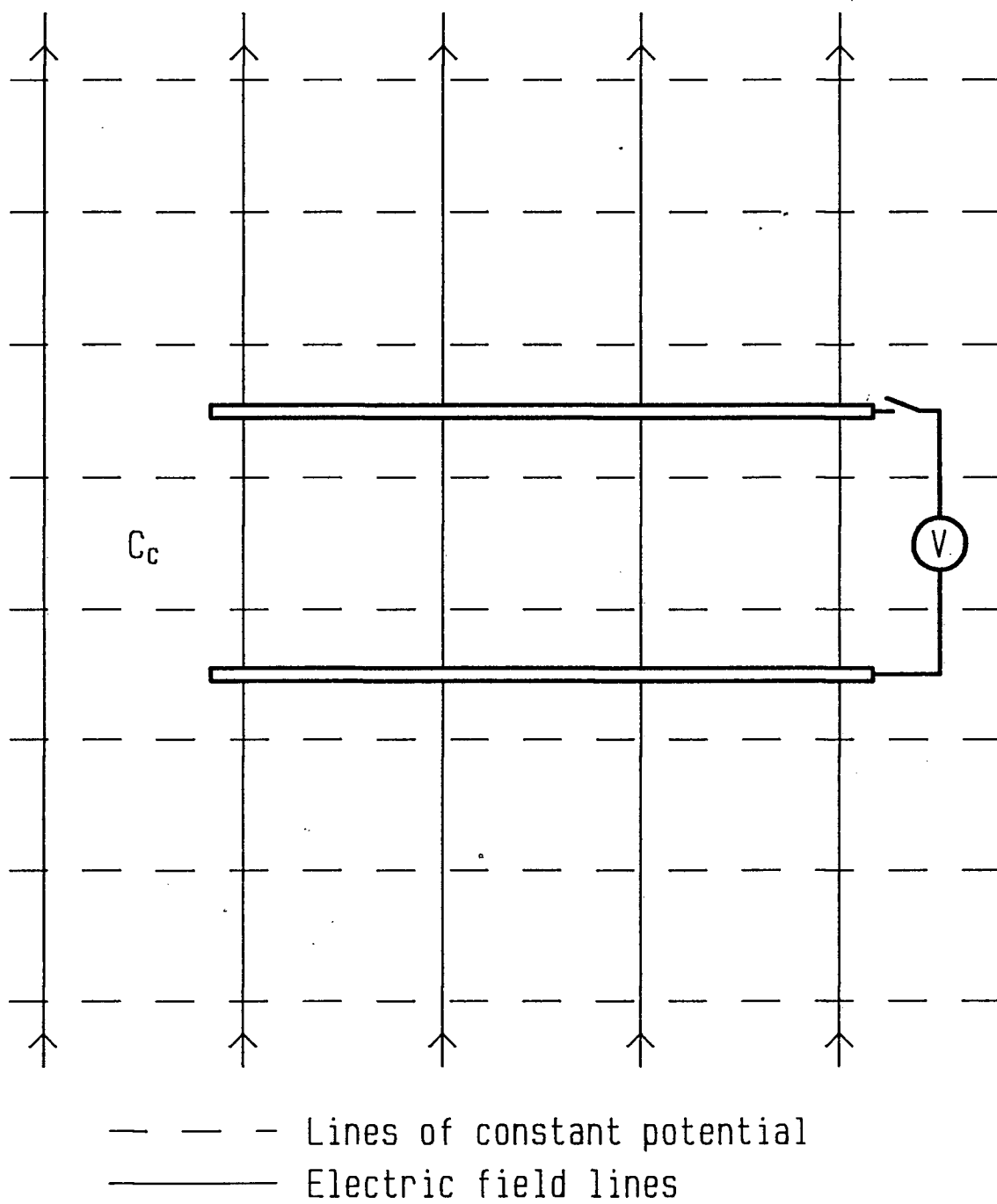


Figure 1

Figure 2 Equivalent circuit of the electric field meter. The charge on the collection capacitor, C_c , can be measured with a nonideal electrometer. The input resistance, R_{in} , the input offset voltage, V_{os} , and the input bias current, I_b , represent the major nonideal characteristics of the electrometer which will affect the electric field measurement. The gain of the electrometer, A , is unity.

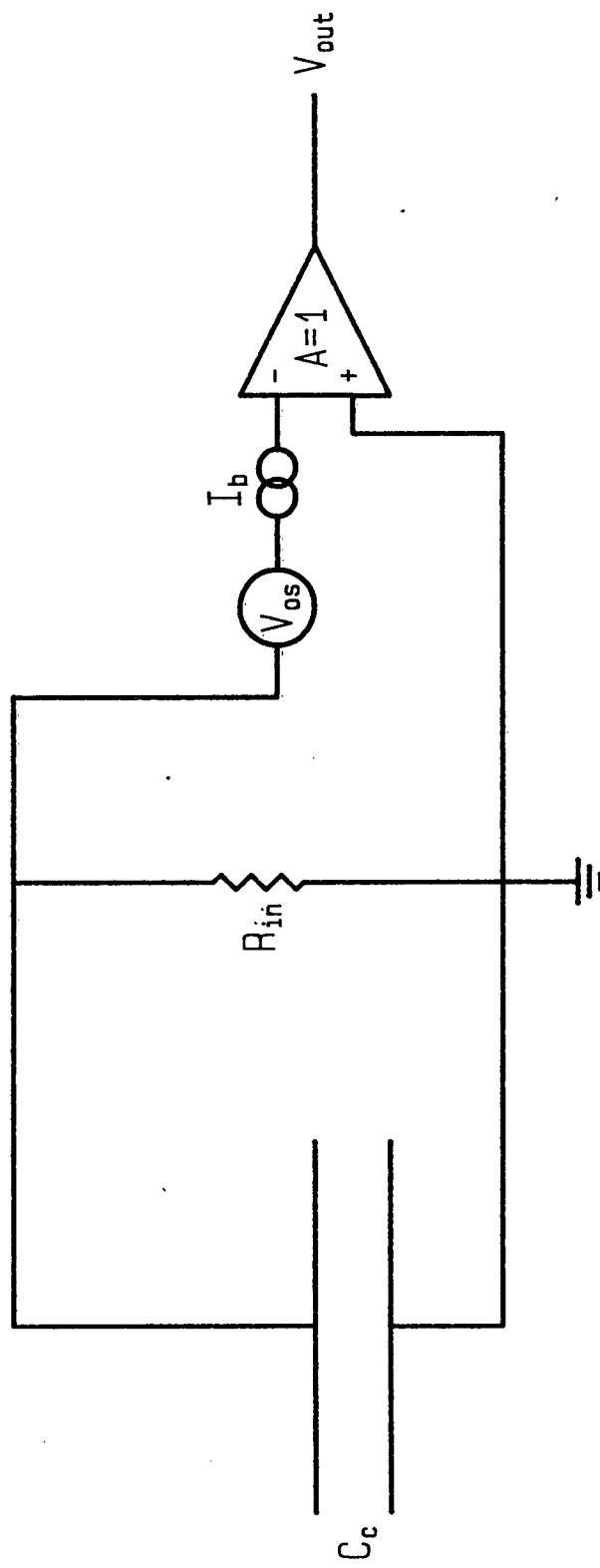
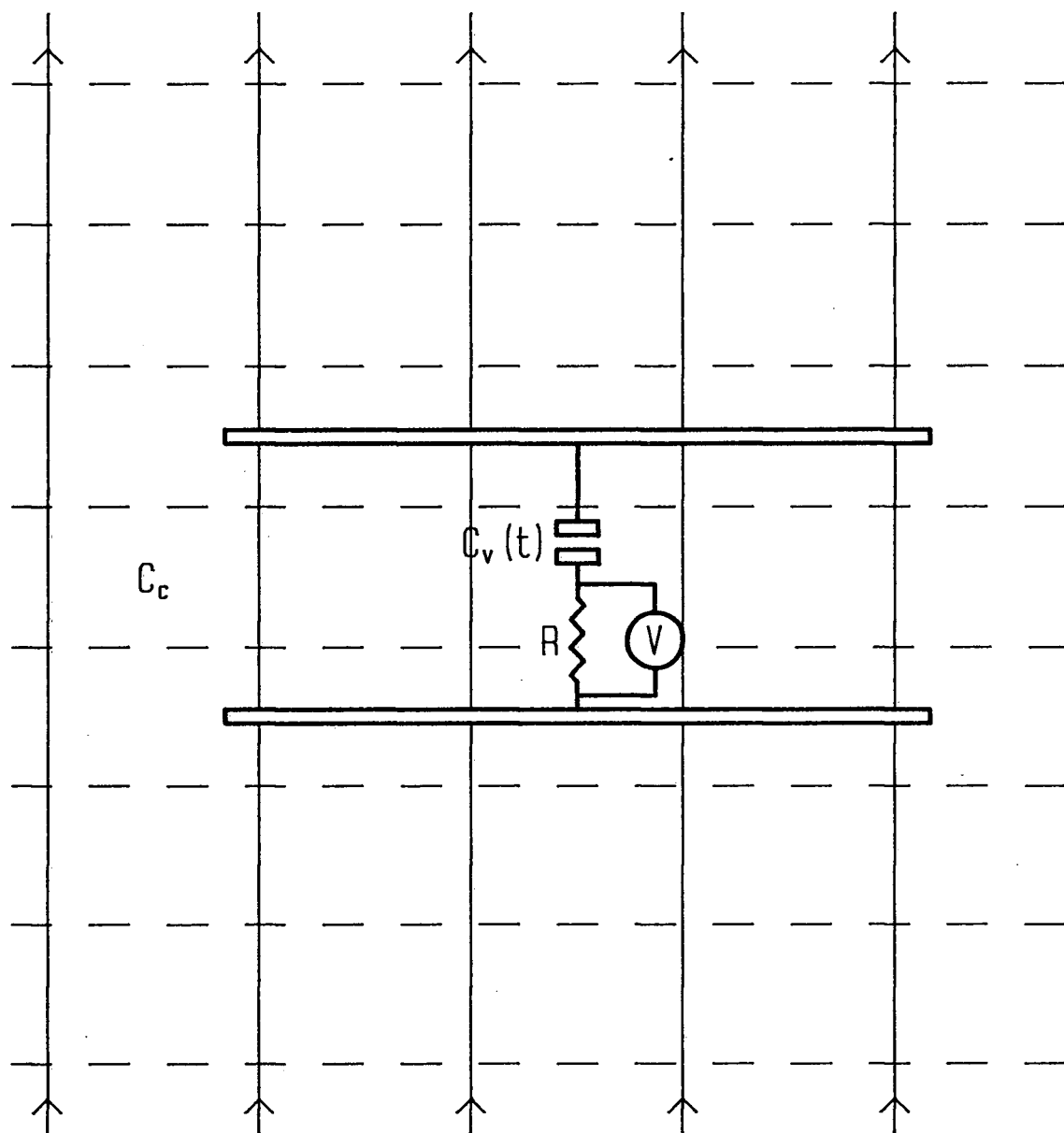


Figure 2

Figure 3 Variable-capacitor modulation circuit. The time varying capacitor, $C_v(t)$, and the collection capacitor, C_c , trap the electric charge induced by the ambient electric field between them. The cycling of the time varying capacitor generates an alternating signal across the load resistor, R , proportional to the ambient electric field.



— — — Lines of constant potential
 ————— Electric field lines

Figure 3

Figure 4 Fluxgate magnetometer operation. The time varying modulation of the relative permeability of the core material immersed in a pseudo-static ambient magnetic field generates a time varying magnetic field near the core. The time varying magnetic field induces a signal into the sense coil surrounding the core. The amplitude of the induced signal is proportional to the strength of the pseudo-static ambient magnetic field. Figures 4(a) and 4(b) show the extreme cases of modulating the relative permeability.

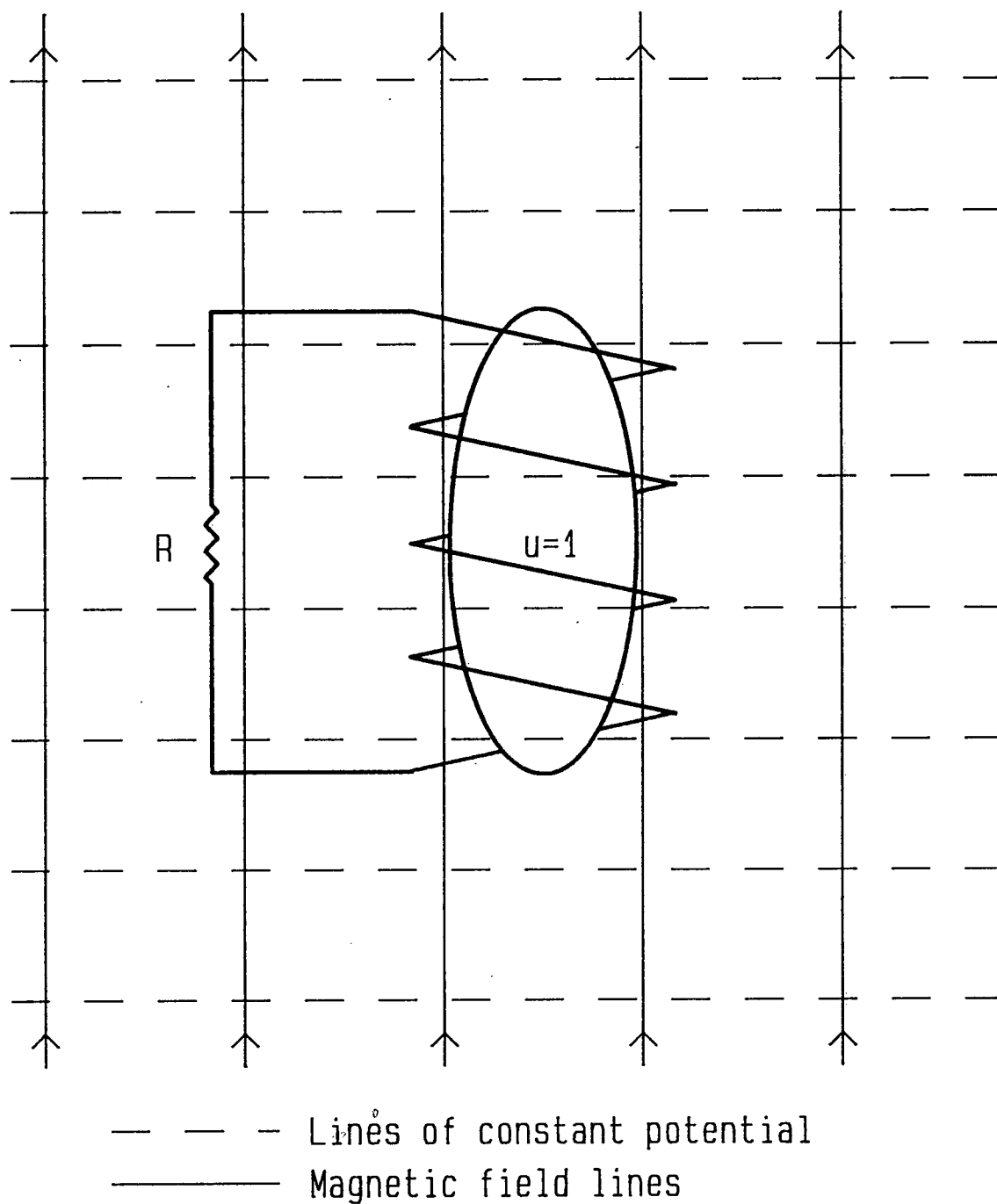


Figure 4(a)

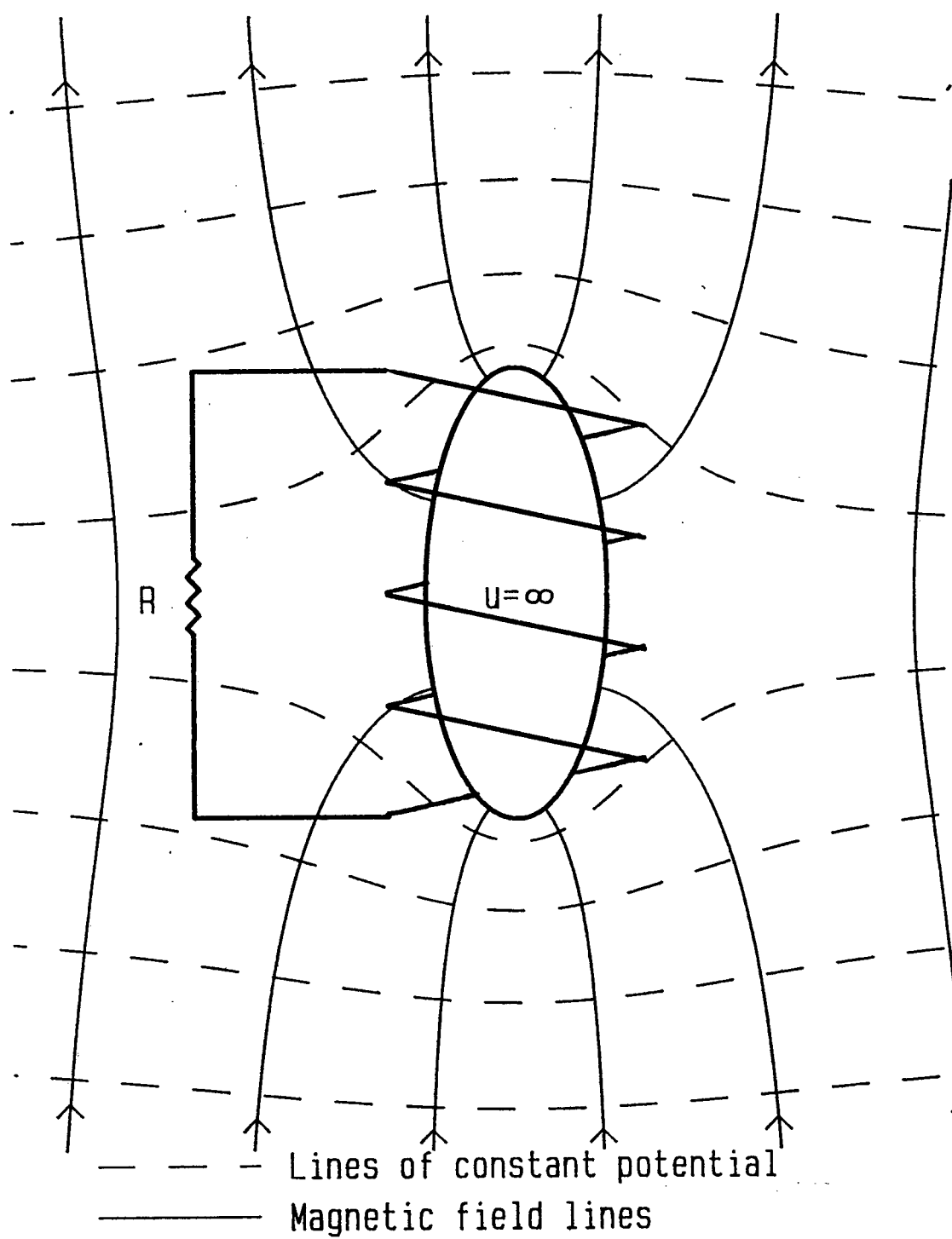


Figure 4 (b)

Figure 5 Variable capacitor configuration. The time varying capacitor is constructed from a matched pair of nonlinear capacitors. The differential drive, balanced about ground, combined with the matched pair of nonlinear capacitors insures the node between the two nonlinear capacitors remains at ground. It also insures that the capacitance varies as a function of the differential drive voltage only.

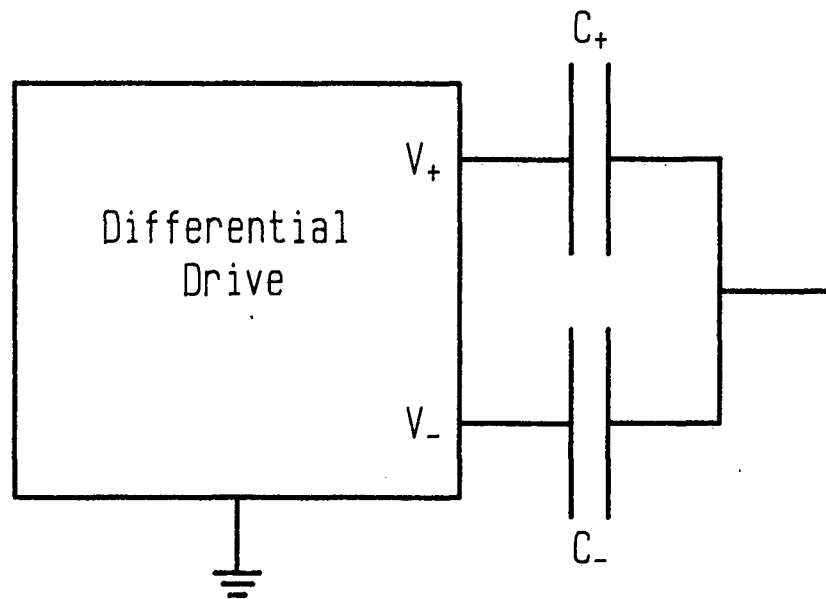


Figure 5

Figure 6 Voltage-versus-capacitance curves for MOSOM capacitors. Figure 6 shows the individual voltage-versus-capacitance curves for the two MOSOM capacitors, C_+ and C_- , used in the prototype. Performance of the fluxgate electric field meter would improve if the capacitance versus voltage curves were better matched.

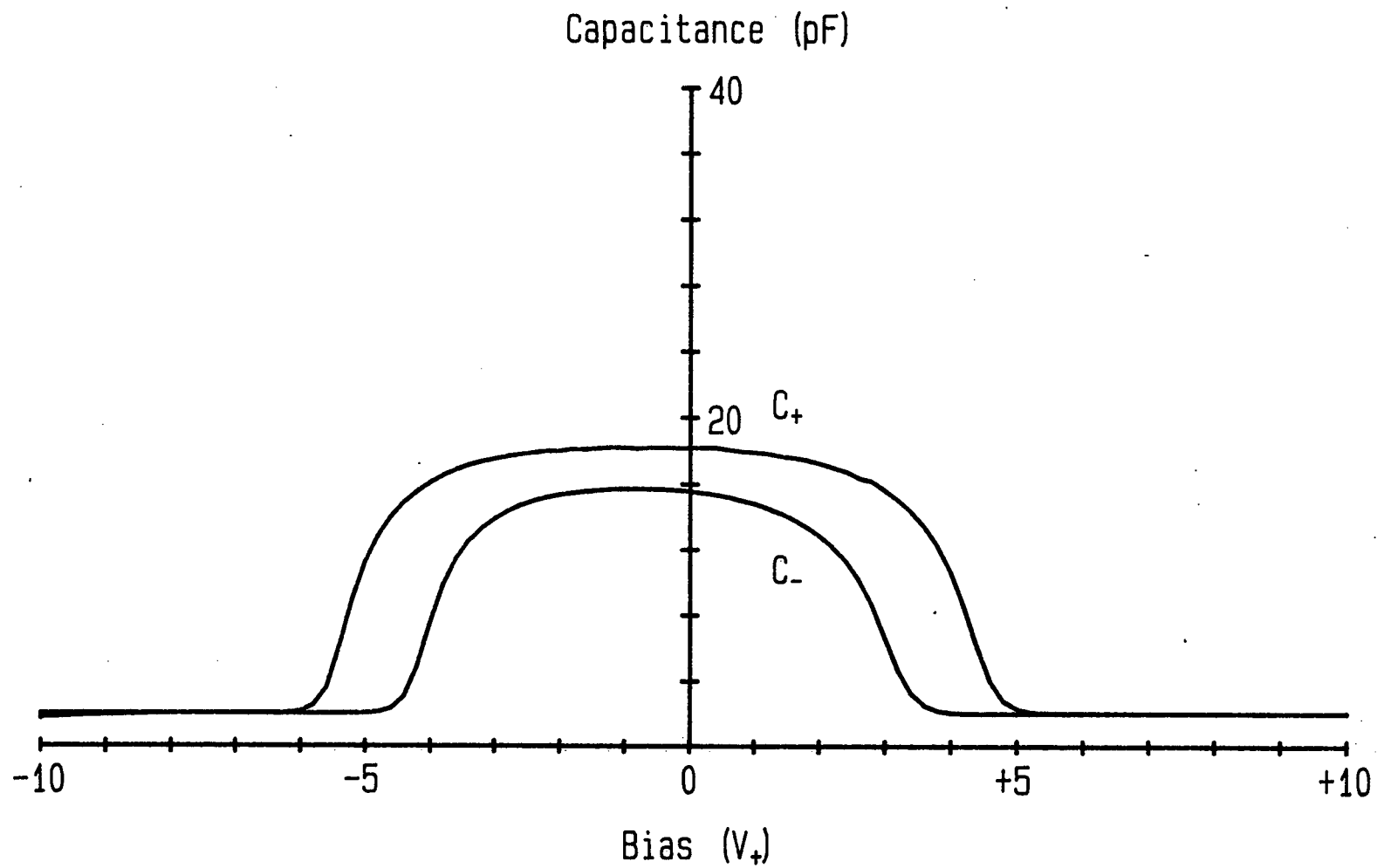


Figure 6

Figure 7 Variation of the time varying capacitor's capacitance. The positive and negative voltage wave forms produced by the differential drive circuit given in Figure 7 are shown. The wave forms produce the displayed time varying capacitance for the time varying capacitor, $C_v(t)$.

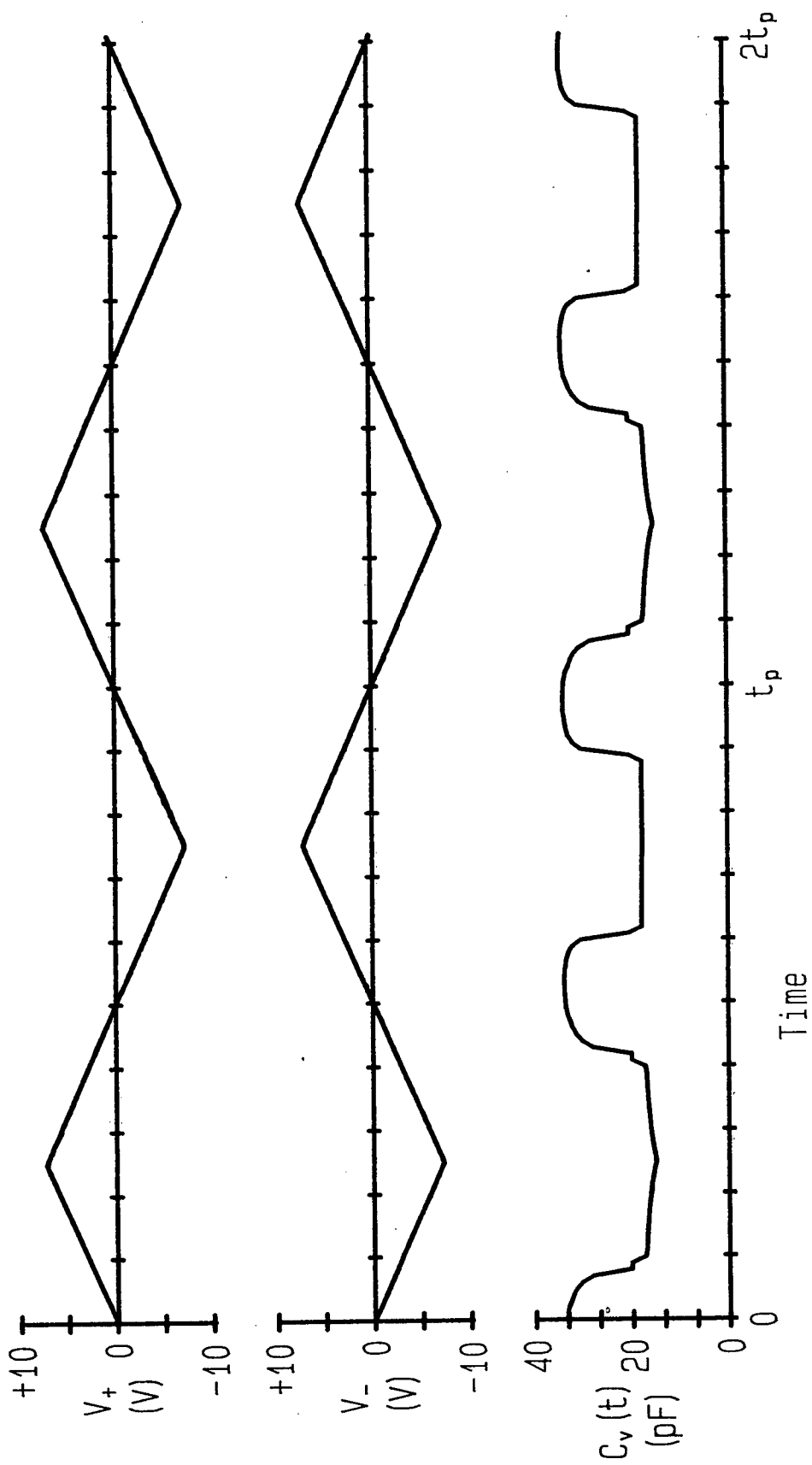


Figure 7

Figure 8 MOSOM nonlinear capacitor design. The nonlinear capacitors used in the construction of the electric field meter consisted of two back to back MOS capacitors. This configuration is referred to as a MOSOM capacitor. The silicon dioxide layer provides an extremely resistive insulating layer.

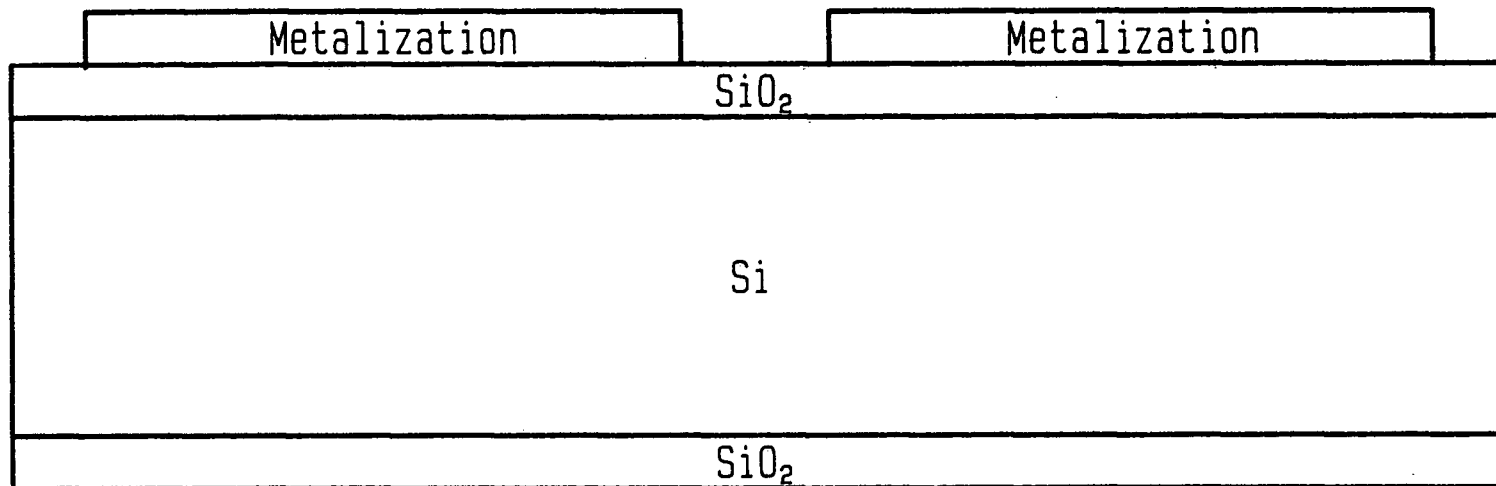
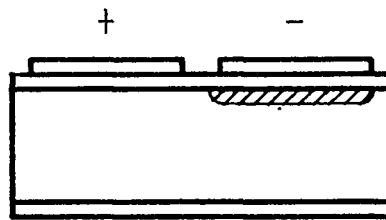
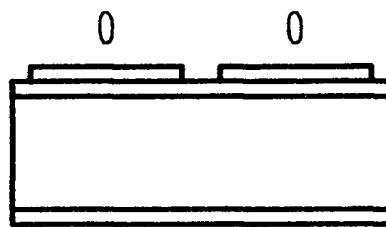


Figure 8

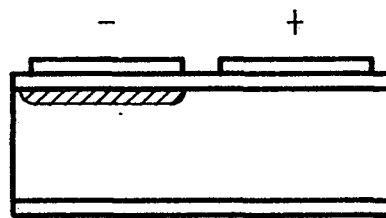
Figure 9 MOSOM nonlinear capacitor operation. Figures 9(a) and (c) show the distribution of the thermally generated electrons in the N type silicon under no electric field. When a potential difference is applied to the areas of metalization, as in Figures 9(b) and (d), depletion regions form. The depletion regions are shown as the hashed areas. Reversal of the drive field destroys the old depletion region and generates a new one.



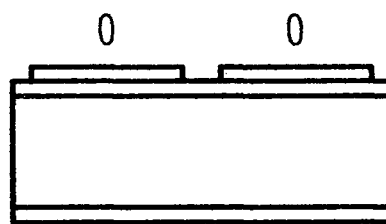
(a)



(b)



(c)



(d)

Figure 9

Figure 10 Variable-capacitor modulator with feedback. The feedback voltage source is placed at the point in the variable-capacitor modulation circuit where it does not cause a low resistance path between the two electrodes of the collection capacitor.

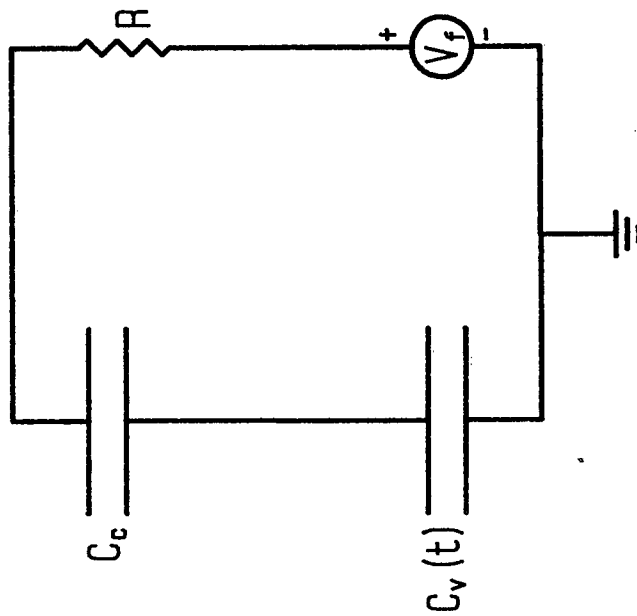


Figure 10

Figure 11 Feedback linearity. The linear relationship between the second harmonic voltage and the feedback voltage is demonstrated by the graph. The slope of the line gives the conversion efficiency which, in this case, has the value 0.10. A $1\text{M}\Omega$ load resistor was used.

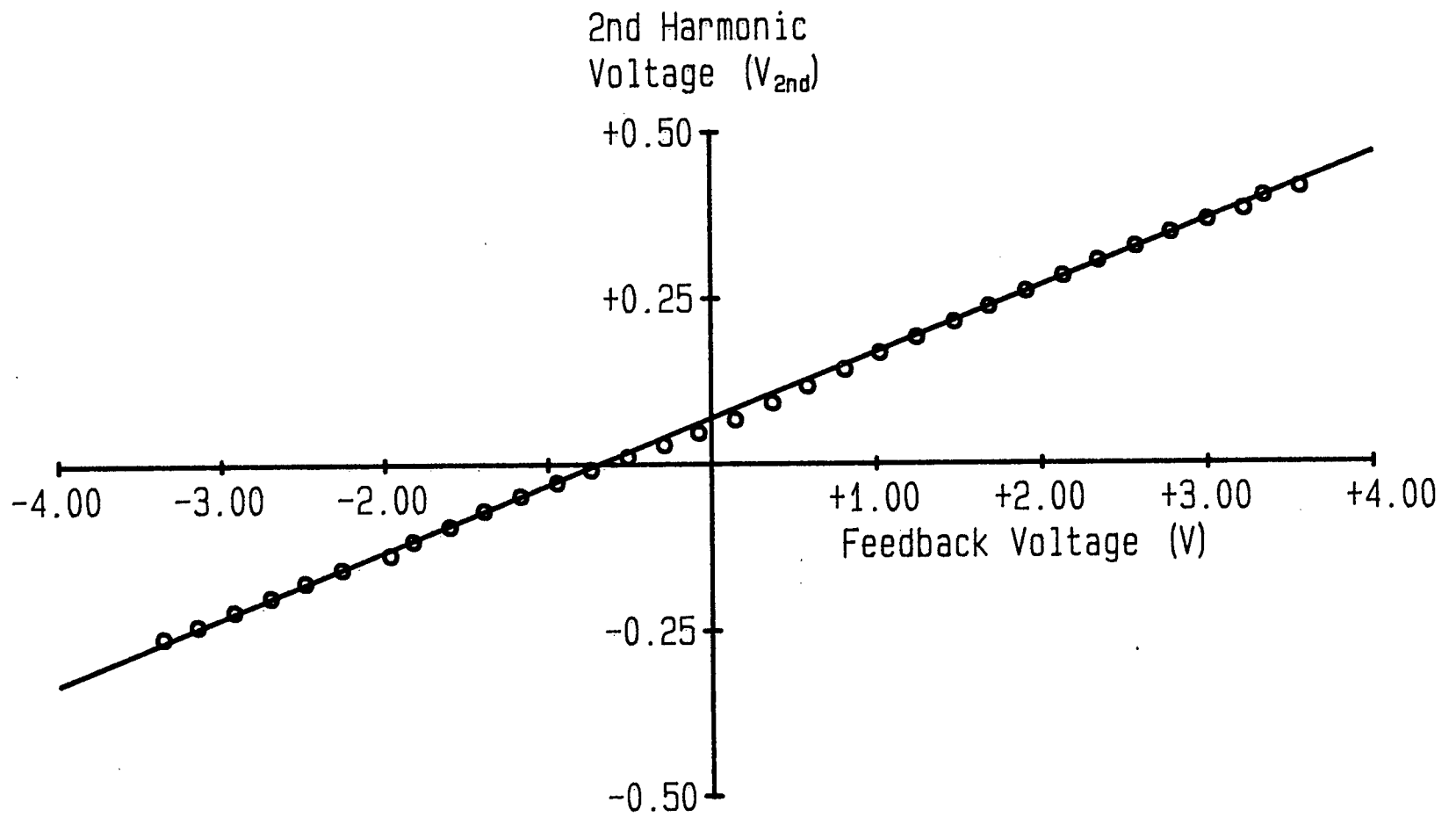


Figure 11

Figure 12 Sensitivity-versus-load resistance curve. This graph compares the predicted and measured conversion efficiency of the fluxgate electric field meter for various load resistances. The small circles indicate the measured values. The solid line represents the predicted conversion efficiency. The discrepancy between the predicted and measured conversion efficiency is discussed in section 5.2.

Conversion
Efficiency

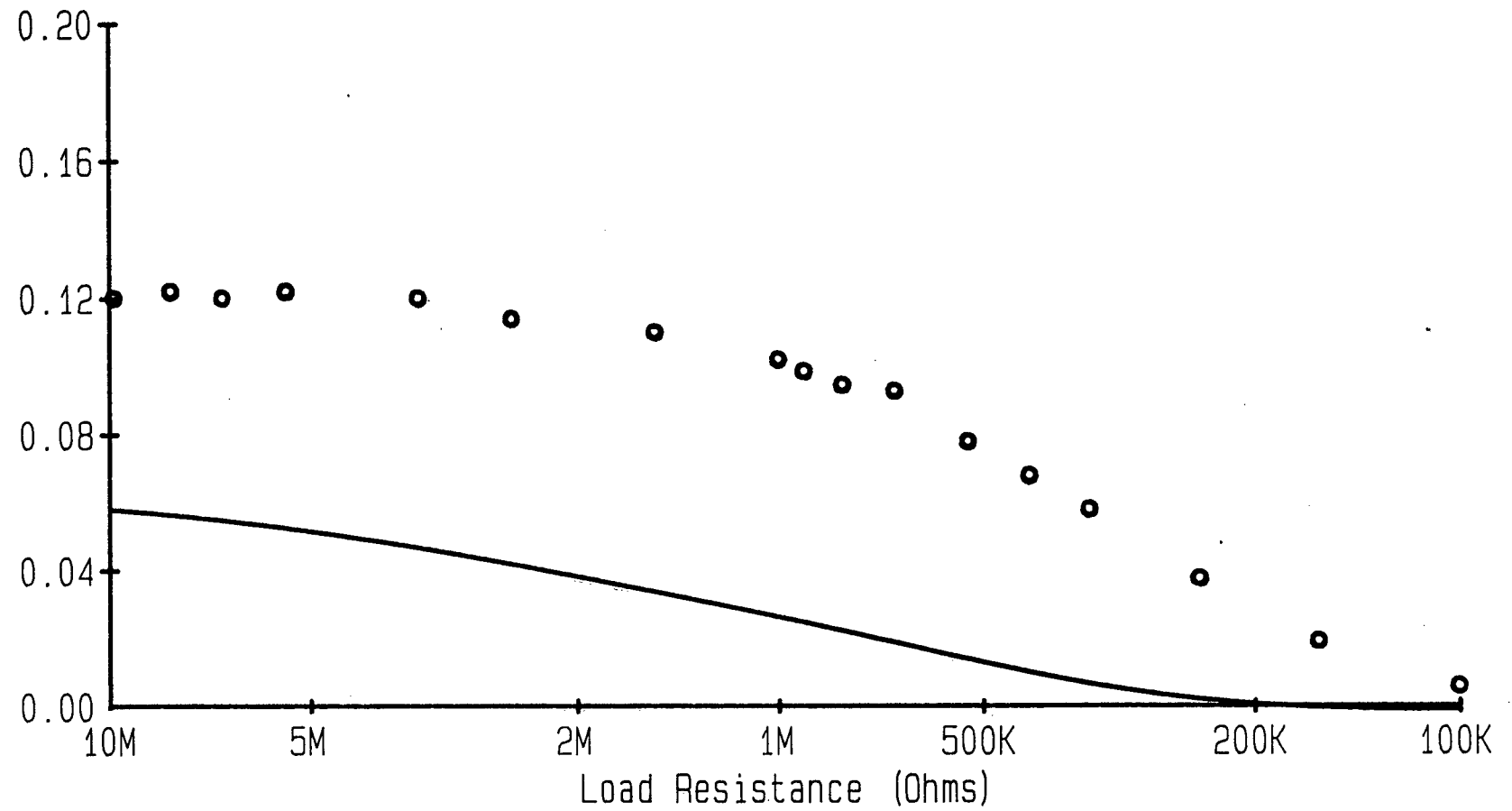


Figure 12

Figure 13 Directionality of instrument. The fluxgate electric field meter shows good directionality. The measured equivalent feedback voltage in a 1Vm^{-1} field at a range of orientations are shown by the small circles. The solid line is a cosine curve with an amplitude of 6.6mV .

Equivalent Feedback
Voltage (mV)

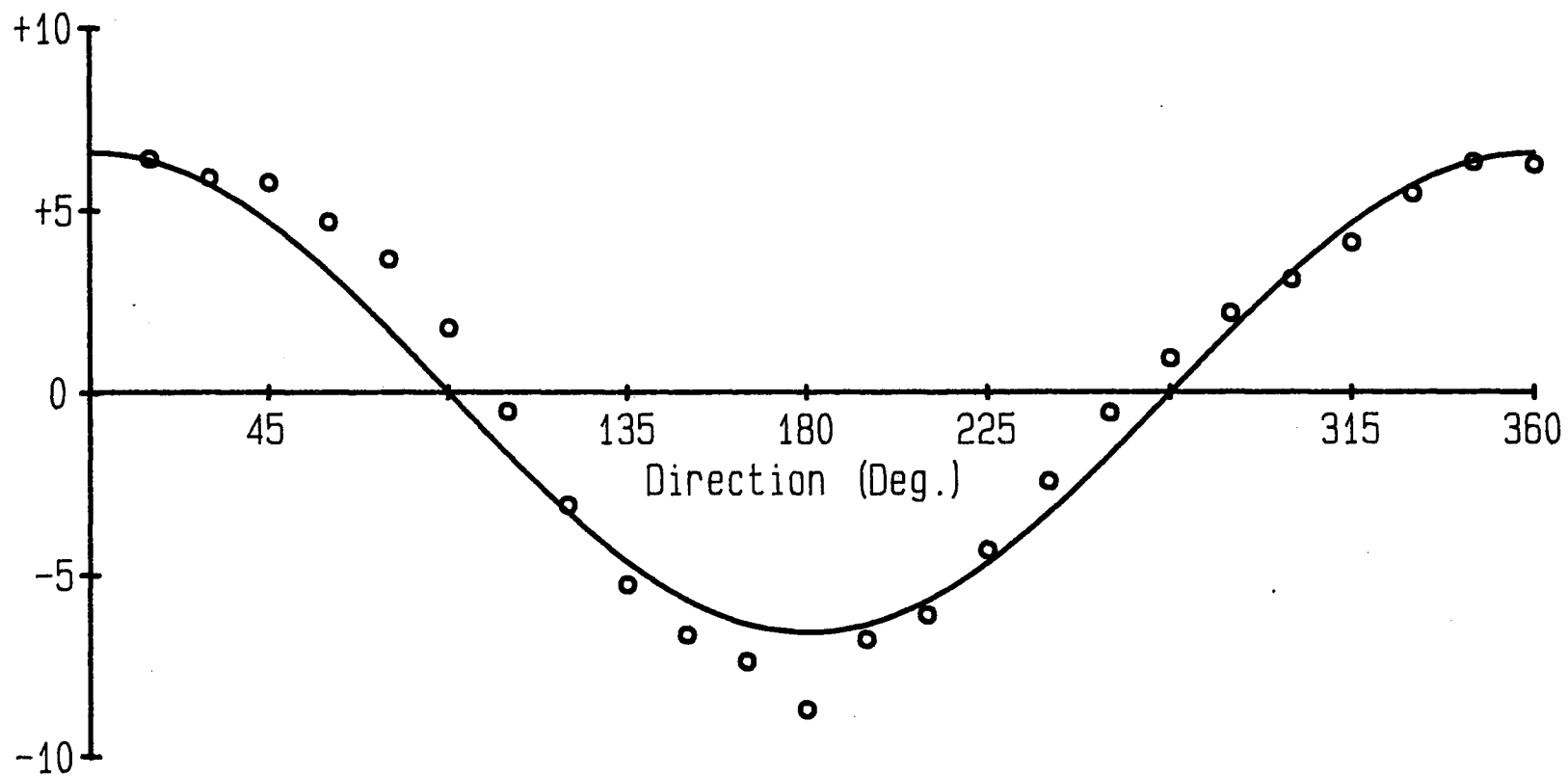


Figure 13

Figure 14 Drift rate. Over time the charge on the collection capacitor drains off. A first the discharge is of a constant current nature. For the 2Ks to 8Ks time period the decay appears to be exponential. The curve approaches the limit of -159mV at large time. Approximately 500 data points compose the displayed curve.

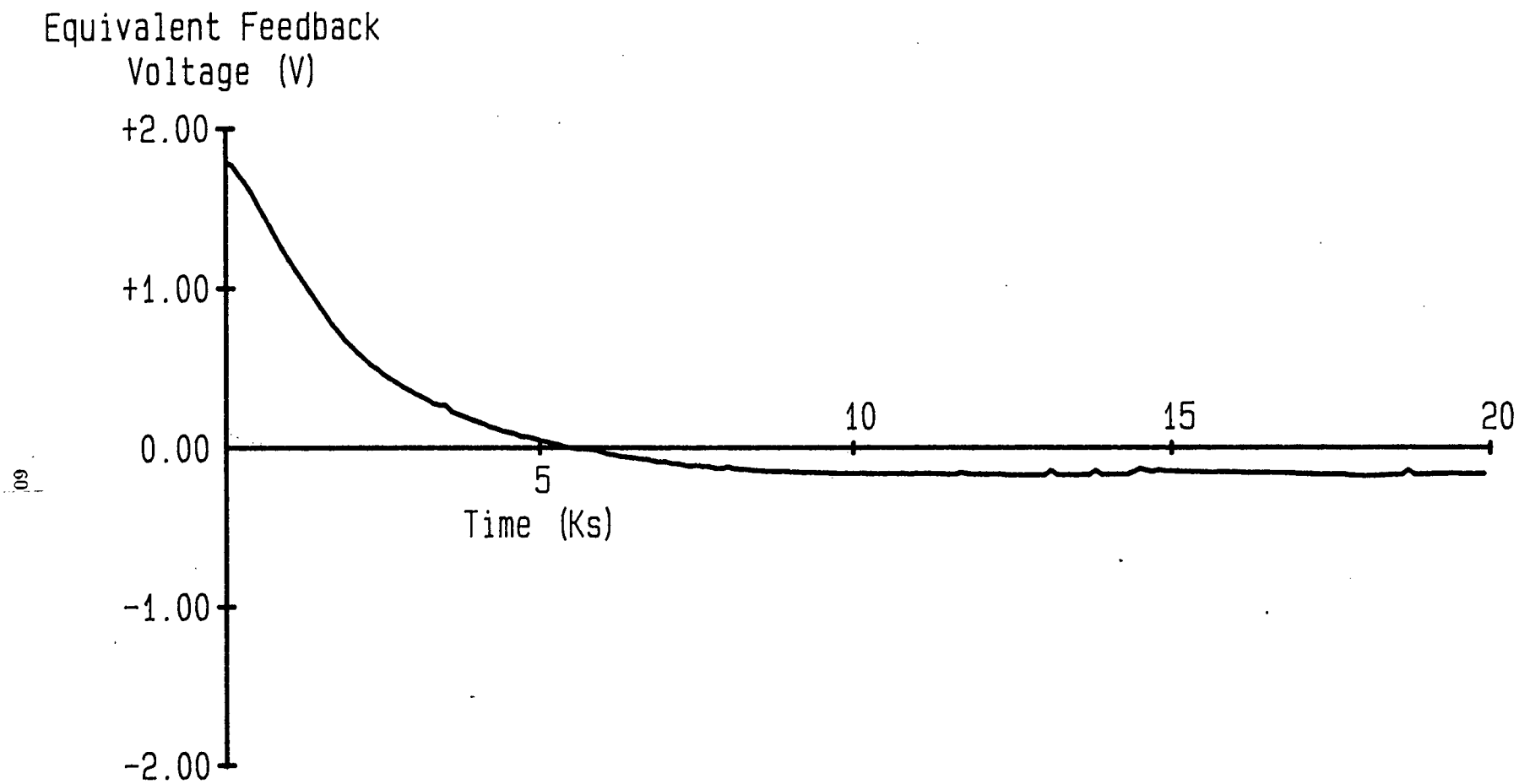


Figure 14

Figure 15 Potential of the instrument. Changing the potential of the sensor with respect to its surroundings also generates an equivalent feedback voltage. The relationship between the equivalent feedback voltage and the field meter potential is shown to be linear.

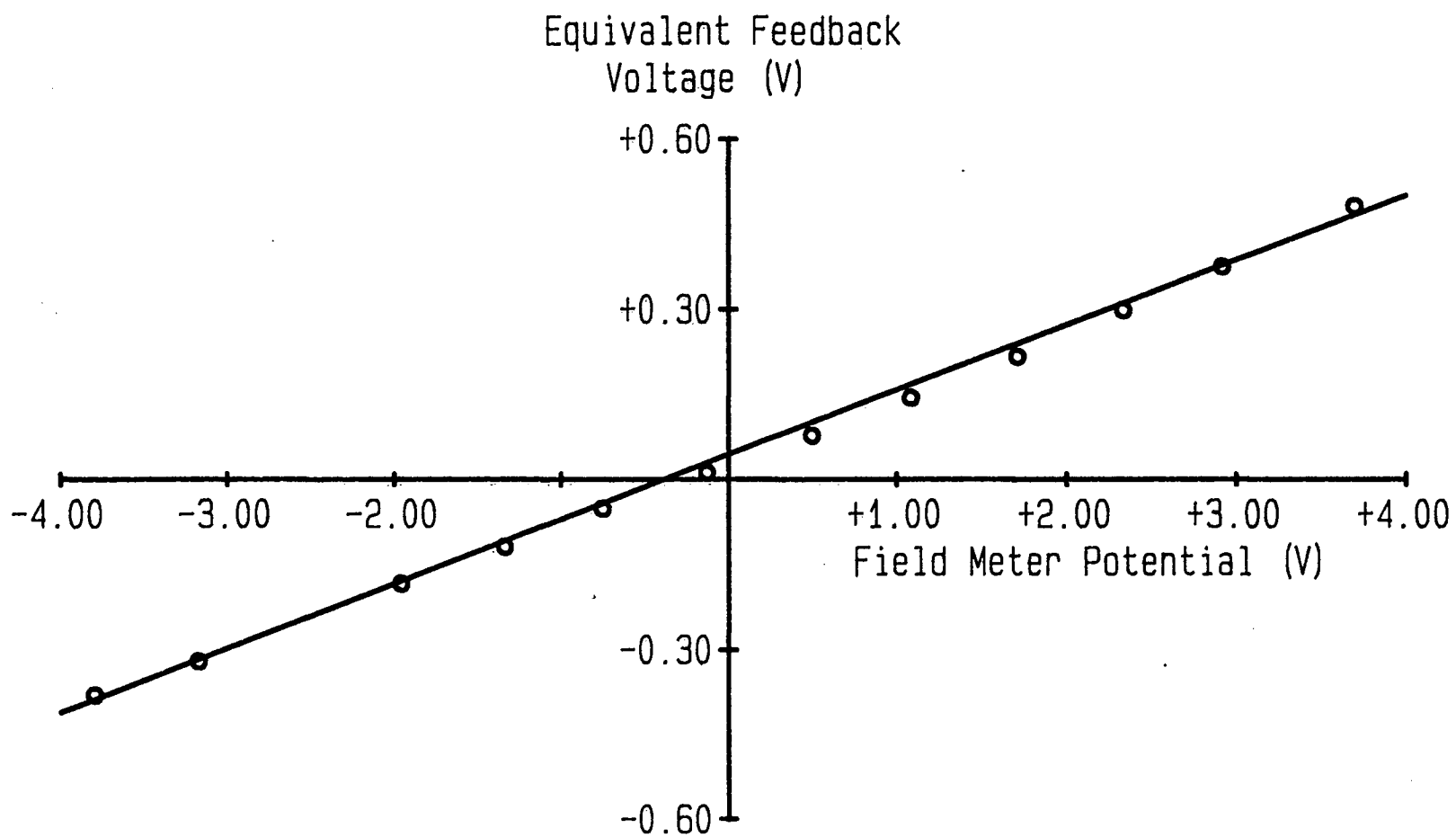


Figure 15

Figure 16 A fluxgate electrometer. The variable-capacitor modulator generates a second harmonic signal across the load resistor, R , which is proportional to the voltage source, V . Ideally the input stage's coupling to ground is purely capacitive thus no charge can leak from the voltage source to ground. The variable-capacitor modulator is configured in the way commonly used by the vibrating-capacitor electrometer.

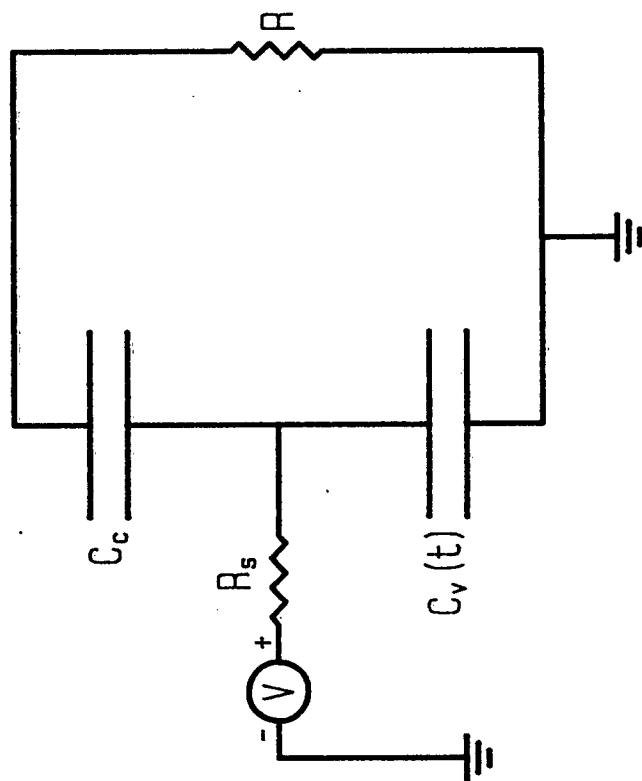


Figure 16

Appendix A Electronic Circuitry of the Instrument

The aim of this thesis was to demonstrate that the fundamental principles of the fluxgate electric fieldmeter are sound. Electronic circuitry with excellent performance specifications was judged to be an unreasonable and unnecessary design goal at this early stage in development of the instrument. Therefore, the major design goals for the electronic circuitry used in the fluxgate electric field meter were to keep the circuitry simple and to get it working. Specifications such as noise, bandwidth, drift rate and gain were of only secondary consideration.

The circuitry of the fluxgate electric field meter can be broken down into three major sections—the clock and drive circuit, the modulation circuit, and the synchronous detector circuit. The clock part of the clock and drive circuit consists of a 1MHz crystal divided down to a 31 250 Hz signal called the second harmonic and a 15 625 Hz signal denoted the fundamental. Both signals have a 50% duty cycle. Figure A1 shows the schematic for the circuit. The second harmonic signal, line 2F, is used by the synchronous detector for synchronization with the drive circuit. The fundamental signal is high-pass filtered to remove its DC component and then integrated to produce a triangular waveform. The triangular wave form is used as the positive side of the differential drive, V_+ . The negative side of the differential drive, V_- , is produced by inverting V_+ . A triangular wave form was chosen to drive the time varying capacitor instead of sinusoidal one because triangular waves are simpler to generate from the square wave fundamental. Sinusoidal waves would have the advantage of having zero energy in harmonics. Zero energy in the harmonics would mean less contamination of the signal in the time varying capacitor by the fluxgate differential drive.

Figure A1 shows 100Ω resistors connecting V_+ and V_- to the 8m long conductors going to the modulation circuit. The reason for these resistors is that the wires going to the modulation circuit are sufficiently long to have a significant amount of capacitance and inductance. This reactive load presented directly to the output stage of the operational amplifiers if the 100Ω resistors were not present, has a destabilizing effect on the amplifiers. The insertion of the 100Ω resistors supplies the necessary damping to stabilize the circuit.

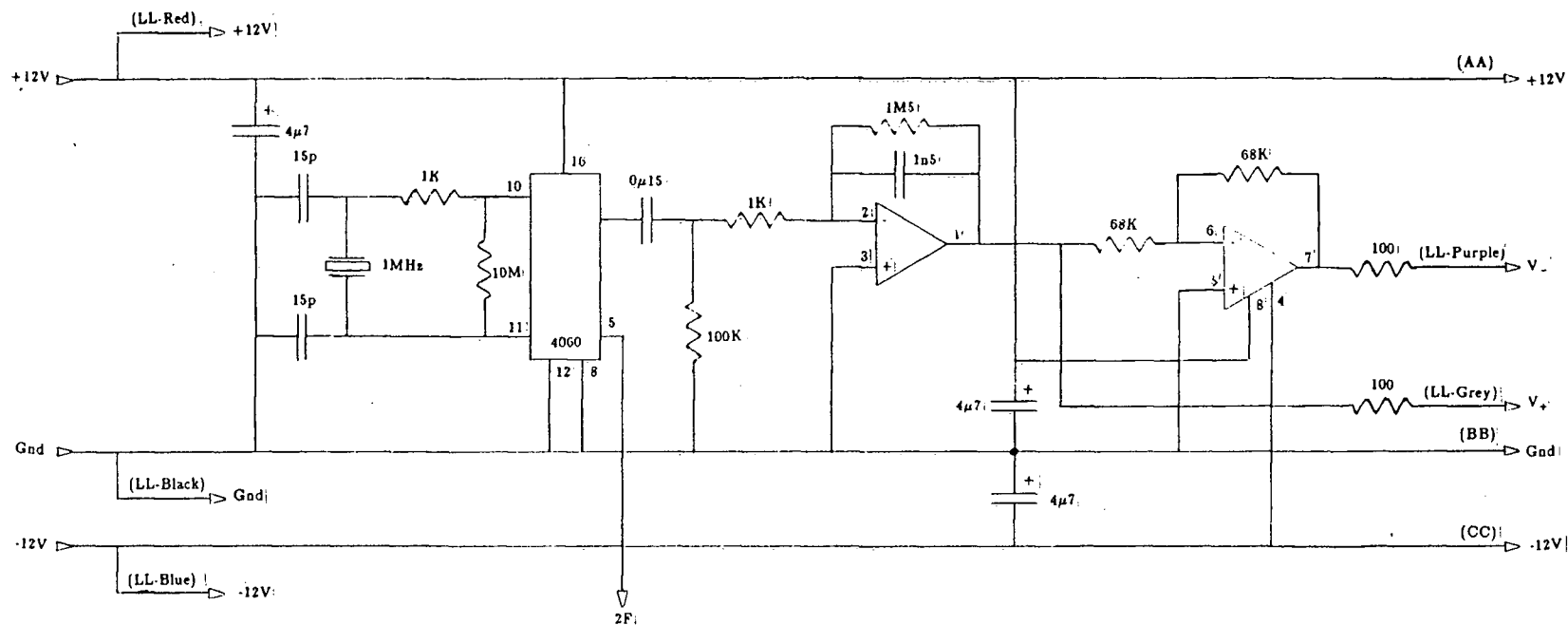
The modulation circuit is the simplest the section of the fluxgate electric field meter. It contains the modulation circuit proper as well as a voltage follower to buffer the signal from the modulation circuit before it is shipped along the 8m long wires to the synchronous detector. Figure A2 supplies a schematic of the circuit. The two nonlinear MOSOM capacitors, C_+ and C_- , and the voltage follower are placed very close to the collection capacitor to reduce the possibility of picking up noise. The feedback voltage, V_f , is supplied to the modulation circuit over the 8m long wires.

The third major section of the fluxgate electric field meter circuitry is the synchronous detector. The circuitry for the synchronous detector, shown in Figure A3, consists of 3 segments—a phase shifter, the synchronous detector proper, and a low-pass filter. The phase shifter is a low-pass integrator with a corner frequency of 8.8kHz. At the second harmonic frequency of 31250 Hz the phase shifter retards the phase by 74.5 degrees and has a gain of 1.46. The purpose of the phase shifter is to shift the phase of the second harmonic signal to a point where it is approximately in phase with the phase sensitive synchronous detector. The synchronous detector produces a DC signal proportional to the amplitude of the in-phase second harmonic signal it receives. The phasing of the synchronous detector is determined

by the second harmonic timing signal, line 2F, from the clock and drive circuit. The synchronous detector also low-pass filters the demodulated signal. The lowpass 3 decibal cutoff is at 150Hz.

The final segment of the synchronous detector section of the fluxgate electric field meter circuitry is a low-pass filter. The low-pass filter is used as an antialias filter before digitizing at the low sampling rates required by some measurements. When high frequency measurements are being made the filter is bypassed. The low-pass filter has a 3 decibel corner at 0.5Hz and a DC gain of unity. The three segments of the synchronous detector combined produce a DC signal which is 4.3 times the root-mean-squared second harmonic signal entering the circuit.

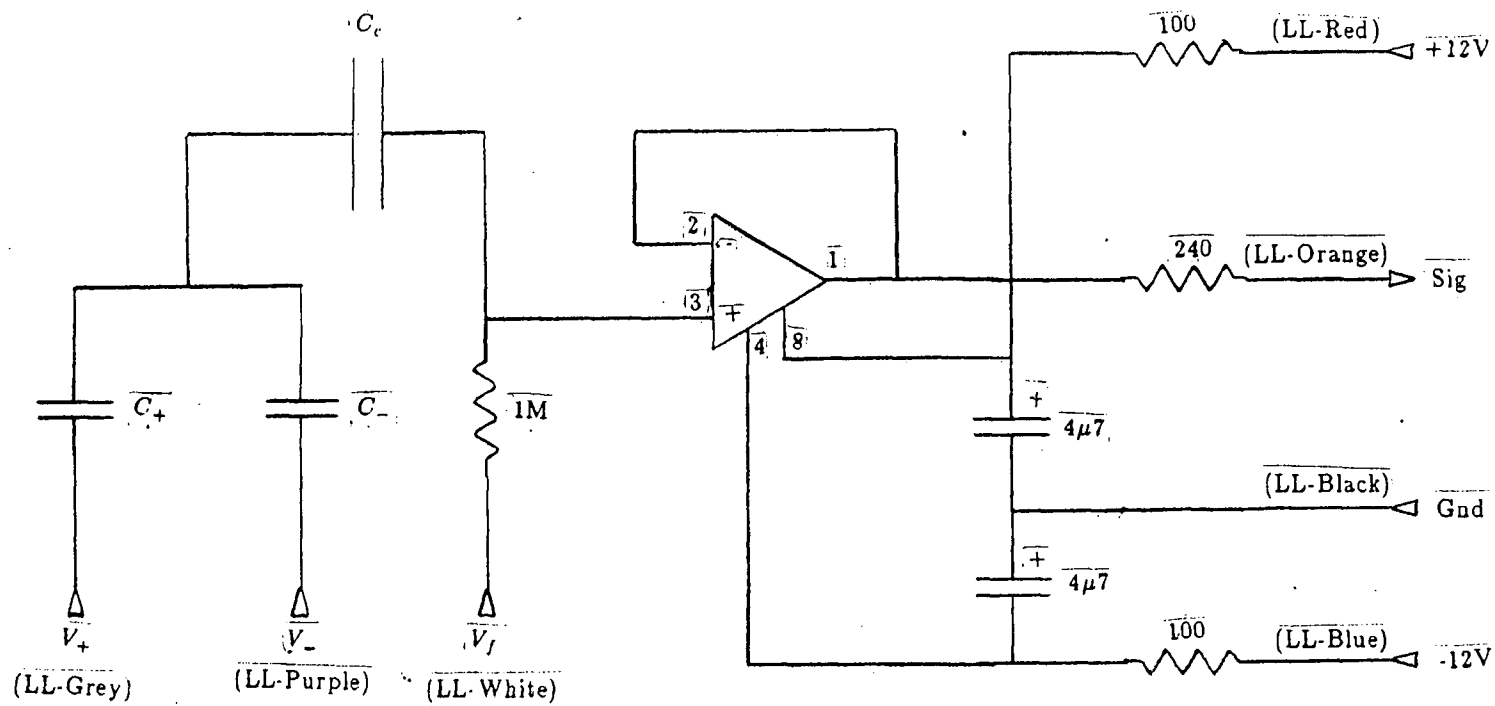
Figure A1 Clock and drive circuit. This circuit supplies the differential drive for the time varying capacitor on lines V_+ and V_- . It also supplies the timing signal for the synchronous detector on line 2F. All resistances are in ohms and all capacitances are in farads. National Semiconductor's LF353 operational amplifier was used exclusively.



Clock and Drive Circuit

Figure A1

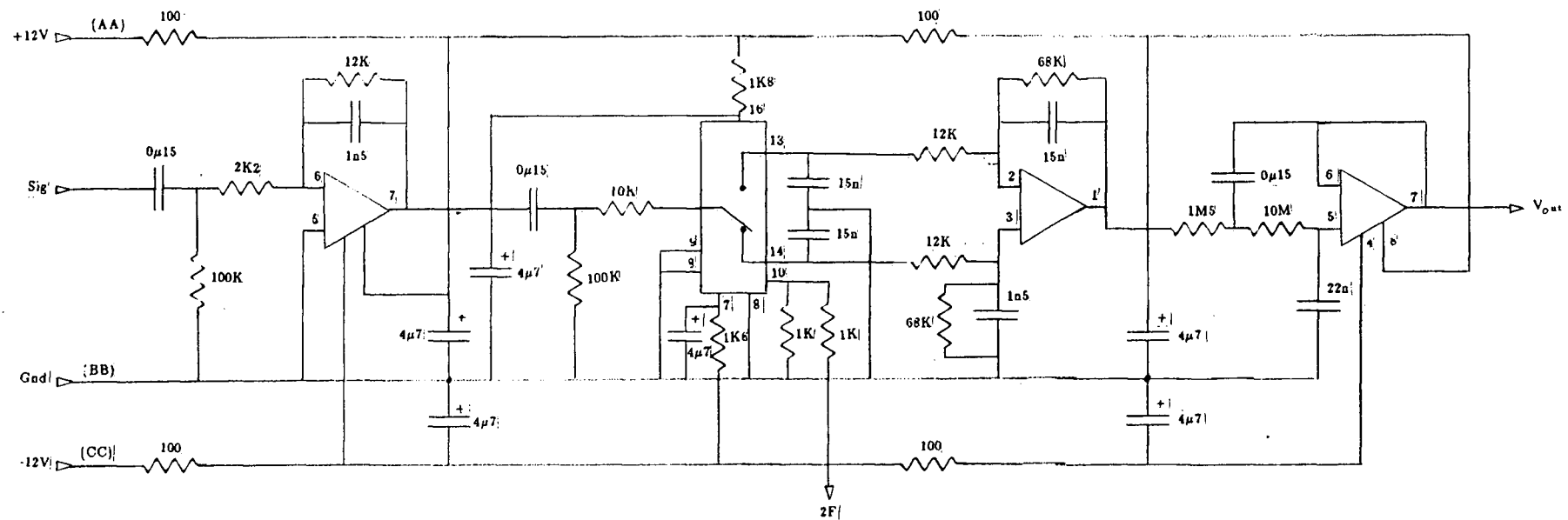
Figure A2 Variable-capacitor modulation circuit. It includes the collection capacitor, C_c , and the nonlinear MOSOM capacitors, C_+ and C_- . The complete circuit shown was immersed in the ambient electric field in the test chamber. All other circuitry was located outside the test chamber and connected to modulation circuit via a 8m long wires. All resistances are in ohms and all capacitances are in farads. National Semiconductor LF353 operational amplifier was used exclusively.



Variable Capacitor Modulation Circuit

Figure A2

Figure A3 Synchronous detector. The synchronous detector circuit is composed of 3 stages. The first stage is an integrator which shifts the second harmonic by ninety degrees to allow synchronous detection. The second stage is the synchronous detector proper. It consists of an single pole double throw switch and a differential amplifier. The third stage is a low-pass filter with a corner frequency of about 0.5Hz and unity gain. All resistances are in ohms and all capacitances are in farads. National Semiconductor's LF353 operational amplifier was used exclusively.



Synchronous Detector

Figure A3

Appendix B Details of the Variable Capacitor

The key to the fluxgate electric field meter was the MOS capacitors used in the MOSOM nonlinear capacitor. For a person experienced in semiconductor fabrication constructing the MOSOM capacitors would be easy; but my complete lack of experience in this area made the task a formidable one for me. Standard fabrication procedures were followed throughout the procedure. Most of the steps in the procedure could mostly likely be improved; but as with the electronic circuitry the main design goal was to keep it simple and get it working.

The steps provided are extremely detailed perhaps to the point of tedium; but I think a comprehensive record is desirable because the MOSOM capacitors are the key component to the fluxgate electric field meter.

See Figure 8 for a diagram of a MOSOM capacitor. The capacitor consists of a structure of

- (1) 2 areas of $1\mu\text{m}$ metalization each 0.5mm^2
- (2) about 200nm SiO_2
- (3) about $200\mu\text{m}$ Si N or P-type
- (4) about 200nm SiO_2 .

The metal used for the metalization was 99.999% pure aluminum. The silicon substrate is a standard 2 inch wafer with $50\Omega\text{m}$ resistivity and is about $200\mu\text{m}$ thick. The last stage of fabrication involved dicing the 2 inch wafer into 1mm by 2mm chips with 2 areas of metalization each. The areas of metalization will be referred to as

gates. Each chip forms one MOSOM capacitor. The N-type silicon was chosen for the substrate because it was available.

The MOSOM capacitor must have no defects under either gate which can conduct electricity through the silicon dioxide layer. Sodium impurities in the silicon dioxide should be kept to very low levels to reduce voltage-versus-capacitance curve drift. All of these characteristics can be obtained by rigorously applying the standard silicon fabrication procedures explained in MOS (Metal-Oxide-Silicon) Physics and Technology by E. H. Nicollian and J. R. Brews (1982, John Wiley and Sons, Inc.)

Fabrication Steps

(1) Perform full RCA cleaning of the silicon wafer except for the last step, which involves immersion in alcohol. RCA cleaning is a standard cleaning procedure for silicon wafers developed by the RCA Corporation. Instead of immersion in alcohol substitute immersion in distilled water. Most alcohols have trace amounts of sodium which can contaminate the silicon dioxide. Distilled water normally does not have these trace amounts of sodium. Make sure the tweezers are clean. Always wear heavy black rubber gloves over light transparent gloves to prevent acid burns. While using acids, always wear at least safety glasses and preferably goggles. Always add acids to water; never, never the reverse! All used acids should be poured slowly down the drain with the city water running at near full volume.

(2) Place the empty oxidization boat in the oxidization oven at a flow of 10% HCl and 90% O₂ for 2 hours to clean the oven and boat thoroughly. Oxidize wafers for 150 minutes at $1150 \pm 10^\circ\text{C}$ in 90% dry O₂ and 10% HCl. Anneal at 1150 in N₂ for 20 minutes. Quick cool in N₂ to prevent oxidization at lower temperatures. After oxidization make sure the HCl line from the tank to the oven is purged with N₂.

This first requires bleeding the HCl out of the line via the oven and then flushing the line with N_2 . The HCl must be completely bled first to prevent the high pressure HCl from flowing into the low pressure N_2 lines.

(3) Deposit $1\mu m$ of very pure Al on the wafer using electron beam evaporation to avoid sodium contamination due to impurities in the filament during thermal evaporation. Make sure the electron beam hits the Al and not the hearth. It can burn through the hearth. Only about half a meter of Al wire should be placed in the hearth as a target. More Al will only cause problems. Post metalize anneal at $400 \pm 10C$ in N_2 for 30 minutes in addition to a 5 minute warm up and a 5 minute cool down period. Anneal might be improved by using H_2 but this can be hazardous.

(4) Place 2 full droppers of positive photoresist on the metalized side of the wafer and spin at 4000 rpm to even out the coating. Soft bake the wafer at $95C$ for 25 minutes. Let the wafer cool for 10 minutes before exposing. Expose the photoresist for 1 min at $30mW/cm^2$ using mask aligner and positive mask. The positive mask consists of an array of $0.5 \times 0.5mm$ black squares on transparent plastic with 1mm spacing between the centers of the squares. Make sure that the cooling nitrogen is always on when the light is on and always make sure to shut the light off 30 minutes before shutting the nitrogen off. Develop in the developing machine making sure the machine is set up for positive photoresist. If the developing machine has just been turned on, run it though one cycle empty to clean out the system. Hard bake the developed photoresist at $125C$ for 25 minutes. The Al still covered with photoresist after developing is protected from dissolution by acid. The Al protected will correspond to the black areas on the positive mask.

Notes on Photoresist:

Positive photoresist is red

Negative photoresist is transparent

Positive photoresist: what ever is exposed goes away

Negative photoresist: what ever is exposed stays

(5) Strip off unprotected Al with fifty-fifty mixture, heated to 65C, of distilled water and phosphoric acid. Strip the photoresist with electronic grade acetone for 5 minutes. The acetone is more effective if heated to 50C but will also work at room temperature. Rinse the wafer for 5 minutes in distilled water. The used acid should be poured slowly down the drain with lots of city water running to dilute the acid. The used acetone should be put into a dirty acetone container. Dice the wafer into $2 \times 1\text{mm}$ chips.

NOTE: The time varying capacitor is a MOS device and can be damaged easily by static charge; therefore proper safety precautions should be taken to avoid static charge. When the time varying capacitor is installed in the electrometer it will often be exposed to large amounts of of static charge therefore it should be made as sturdy as possible.